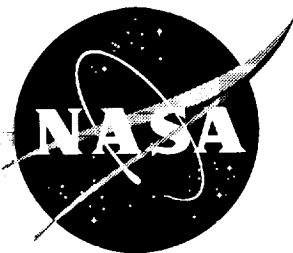


NASA/CR-2000-210314



# On the Coupling of CDISC Design Method With FPX Rotor Code

*Hong Hu*  
*Hampton University, Hampton, Virginia*

---

December 2000

## The NASA STI Program Office ... in Profile

Since its founding, NASA has been dedicated to the advancement of aeronautics and space science. The NASA Scientific and Technical Information (STI) Program Office plays a key part in helping NASA maintain this important role.

The NASA STI Program Office is operated by Langley Research Center, the lead center for NASA's scientific and technical information. The NASA STI Program Office provides access to the NASA STI Database, the largest collection of aeronautical and space science STI in the world. The Program Office is also NASA's institutional mechanism for disseminating the results of its research and development activities. These results are published by NASA in the NASA STI Report Series, which includes the following report types:

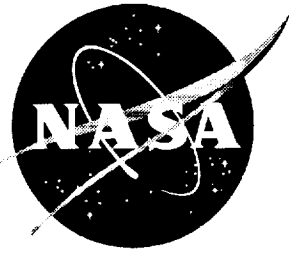
- **TECHNICAL PUBLICATION.** Reports of completed research or a major significant phase of research that present the results of NASA programs and include extensive data or theoretical analysis. Includes compilations of significant scientific and technical data and information deemed to be of continuing reference value. NASA counterpart of peer-reviewed formal professional papers, but having less stringent limitations on manuscript length and extent of graphic presentations.
- **TECHNICAL MEMORANDUM.** Scientific and technical findings that are preliminary or of specialized interest, e.g., quick release reports, working papers, and bibliographies that contain minimal annotation. Does not contain extensive analysis.
- **CONTRACTOR REPORT.** Scientific and technical findings by NASA-sponsored contractors and grantees.
- **CONFERENCE PUBLICATION.** Collected papers from scientific and technical conferences, symposia, seminars, or other meetings sponsored or co-sponsored by NASA.
- **SPECIAL PUBLICATION.** Scientific, technical, or historical information from NASA programs, projects, and missions, often concerned with subjects having substantial public interest.
- **TECHNICAL TRANSLATION.** English-language translations of foreign scientific and technical material pertinent to NASA's mission.

Specialized services that complement the STI Program Office's diverse offerings include creating custom thesauri, building customized databases, organizing and publishing research results ... even providing videos.

For more information about the NASA STI Program Office, see the following:

- Access the NASA STI Program Home Page at <http://www.sti.nasa.gov>
- E-mail your question via the Internet to [help@sti.nasa.gov](mailto:help@sti.nasa.gov)
- Fax your question to the NASA STI Help Desk at (301) 621-0134
- Phone the NASA STI Help Desk at (301) 621-0390
- Write to:  
NASA STI Help Desk  
NASA Center for AeroSpace Information  
7121 Standard Drive  
Hanover, MD 21076-1320

NASA/CR-2000-210314



# On the Coupling of CDISC Design Method With FPX Rotor Code

*Hong Hu  
Hampton University, Hampton, Virginia*

National Aeronautics and  
Space Administration

Langley Research Center  
Hampton, Virginia 23681-2199

Prepared for Langley Research Center  
under Contract NAS1-19935

---

December 2000

---

Available from: \_\_\_\_\_

**NASA Center for AeroSpace Information (CASI)** ✓  
7121 Standard Drive  
Hanover, MD 21076-1320  
(301) 621-0390

**National Technical Information Service (NTIS)**  
5285 Port Royal Road  
Springfield, VA 22161-2171  
(703) 605-6000

## **PREFACE**

The work presented in this report is performed under contract NAS 1-19935, Task No. 15 from National Aeronautics and Space Administration, Langley Research Center. Dr. Henry E. Jones is the Technical Monitor. The author would like to express his appreciation to Dr. Henry E. Jones for providing many helpful suggestions during the entire investigation, and to Dr. Richard L. Campbell for providing the newest version of the CDISC code and useful discussion about the code.

## CONTENTS

	<u>Page</u>
PREFACE	i
Summary	1
1. Introduction	2
2. The CDISC Method	2
3. The FPX Rotor Code	4
4. Implementation	5
5. Results	6
5.1 Basic DISC Results	6
5.2 CDISC Results	7
6. Conclusions	8
References	33

# **On the Coupling of CDISC Design Method with FPX Rotor Code**

by

Hong Hu

Hampton University  
Hampton, Virginia 23668

## **Summary**

A rotor section aerodynamic design package is developed by coupling Constrained Direct Iterative Surface Curvature (CDISC) design method with FPX rotor code. The coupling between the CDISC design and the FPX flow analysis is fully automated. The CDISC design method employs a predictor-corrector procedure iteratively to determine a surface geometry which produces a target pressure distribution, where target pressure distribution is either pre-defined or automatically generated through flow and geometry constraints. The FPX code is an eXtended Full-Potential rotor Computational Fluid Dynamics (CFD) code, which solves three-dimensional unsteady full-potential equation in a strong conservative form using an implicit approximate-factorization finite-difference scheme with entropy and viscosity corrections. Application of the CDISC design method coupled with the FPX rotor code is made for rotor blades in hovering motions. Several design examples are presented to demonstrate the capability and efficiency of the new package in rotor section design.

## 1. Introduction

The recent advances in Computational Fluid Dynamics (CFD) have provided accurate and detailed flow solutions in an efficient way. These advances have generated interest in integrating CFD code into design methods. Automated aerodynamic design methods are beginning to become part of this process. These methods can be divided into two general categories: inverse methods that use an inverse solver, and predictor-corrector methods that use a direct flow analysis in an iterative manner. The predictor-corrector methods can be coupled with any flow solver and hence take advantage of the advances in Computational Fluid Dynamics.

The Constrained Direct Iterative Surface Curvature (CDISC) design method of Campbell and Smith<sup>1</sup> and Campbell<sup>2</sup> is a pressure based predictor-corrector design method. The CDISC method determines a surface geometry which produces a target pressure distribution, where target pressure distribution is either pre-defined or automatically generated through flow and geometry constraints. The method has been coupled with several advanced CFD flow solvers<sup>1-5</sup> for fixed-wing section design, including design in the presence of nacelles. Results from these codes indicate that the CDISC method is robust and accurate.

This report presents the coupling of the CDISC method with a rotor Computational Fluid Dynamics code - the FPX code. As the best of author's knowledge, this is the first time on using the CDISC method in helicopter rotor section design. In the next few sections, a brief description of the CDISC method and the FPX rotor CFD code is given, which is followed by the implementation of their coupling. Finally, several design examples are presented to demonstrate the capability and efficiency of the new design package in rotor section design.

## 2. The CDISC Method

The Constrained DISC method (CDISC method) is an extension of the basic DISC method. The DISC method employs a pressure based predictor-corrector design procedure, where the calculated surface pressure distribution is compared with a target distribution and the correction to surface geometry is then made to achieve the target pressure distribution. In more detail, the DISC method starts with an initial surface geometry and flow condition at design point, a flow analysis code is used to generate surface pressure distribution. The calculated pressure distributions are then compared with the target distribution and the difference gives the correction to the surface geometry through a design module. A new geometry is obtained and the flow analysis code is used again to generate a new surface pressure distribution until the target pressure distribution is achieved.

The DISC design module relates the difference between the calculated and the target



surface pressure coefficients ( $\Delta C_p$ ) to the change in surface curvature ( $\Delta C$ ) at a given chordwise location. Different modules are used in different regions during the design process. For subsonic and low supercritical flows where a small change in surface geometry can only result in a small change in surface pressure, the relationship is derived<sup>1</sup> from the momentum equation as

$$\Delta C = A(1 + C^2)^B \Delta C_p \quad (1)$$

where  $A$  is 1 for the upper surface and  $-1$  for the lower surface;  $B$  is input constant ranging from 0.0 to 0.5, with the higher values giving faster convergence but decreasing the numerical stability; and  $C$  is streamline curvature at aerodynamic surface. For the moderate to high supercritical flows where a small change in surface geometry can cause a large change in surface pressure coefficients, the relationship is obtained<sup>1</sup> from supersonic thin airfoil equation as

$$\Delta C = \frac{d(\Delta C_p)}{dx} \frac{A\sqrt{M_\infty^2 - 1}}{2} \frac{1}{[1 + (dy/dx)^2]^{1.5}} \quad (2)$$

where  $y$  defines airfoil surface.

The advantage of the DISC method over the inverse method is that the method can be treated as a “black box”. The “black box” can be incorporated into any CFD code, and thus take the advantage of the advances of CFD.

The Constrained DISC method specifies desirable characteristics of the target pressure distribution. The target pressure is automatically generated and updated at each step based on the specified characteristics - the constraints. The typical flow constraints are lift, drag, pitching moment and pressure gradient. The typical geometry constraints are airfoil maximum/minimum thickness and leading edge radius, and so on. Including geometry constraints in the design process will yield an airfoil/wing/rotor blade that not only satisfies target pressure distributions but also be practical to build. In the CDISC design method, constraints are easily included in the design process to satisfy various design requirements. For example, upper and lower surfaces can be designed individually and therefore designing only one surface is possible, which is very useful in design of very thin airfoil sections. Partial surface design is an option. Surface smoothing eliminates sharp changes in surface curvature. The limitation of surface curvature is useful in highly cambered airfoil section design.

The three-dimensional (3D) wing/rotor blade design is considered as a set of airfoil section design problems at specified span-locations. For 3D span-load distribution design, the DISC method can also be used by modifying twist distributions. For simultaneous airfoil section and span-load distribution design, the surface curvature and twist modification methods can be used together. The CDISC design method has been shown to be comprehensive and easy to use, it is therefore highly desirable to use the method in various

configuration design problems. In the present work, the CDISC is used for helicopter rotor section design when coupled with a rotor CFD code.

### 3. The FPX Rotor Code

While in the fixed-wing aerodynamic computational community more and more expensive and complex Euler and Navier-Stokes methods are used recently, potential methods still serve as a major analysis tool in the rotary-wing aerodynamic computational community. The eXtended Full-Potential (FPX) rotor code<sup>6</sup> is one such accurate and efficient potential method, which represents an industry standard for rotary-wing computations. The FPX code is a modified and enhanced version of Full-Potential Rotor (FPR) code<sup>7</sup>. The code (either FPR or FPX) has been used in various helicopter hover and forward flight cases, including Blade-Vortex Interaction (BVI) calculations<sup>8</sup>, nonlinear acoustic analysis<sup>9</sup> and coupling with the comprehensive helicopter code CAMRAD<sup>10</sup>. The application of the code produces excellent results. The code is also highly optimized and a typical steady run takes 1-7 minutes on a Cray-C90 supercomputer with a single processor.

The FPX/FPR codes solve the unsteady three-dimensional full-potential equation in a strong conservation form using an implicit finite-difference scheme for flow around rotor blade. It is less expensive than either Euler or Navier-Stokes methods, and yet produces accurate solutions for various helicopter flows without significant separations.

The unsteady, three-dimensional full-potential equation in strong conservation form in blade-fixed body-conforming coordinates  $(\xi, \eta, \zeta, \tau)$  is written as

$$\frac{\partial}{\partial \tau} \left( \frac{\rho}{J} \right) + \frac{\partial}{\partial \xi} \left( \frac{\rho U}{J} \right) + \frac{\partial}{\partial \eta} \left( \frac{\rho V}{J} \right) + \frac{\partial}{\partial \zeta} \left( \frac{\rho W}{J} \right) = 0 \quad (3)$$

with

$$\rho = \left\{ 1 + \frac{\gamma - 1}{2} [-2\Phi_\tau - (U + \xi_t)\Phi_\xi - (V + \eta_t)\Phi_\eta - (W + \zeta_t)\Phi_\zeta] \right\}^{\frac{1}{\gamma-1}} \quad (4)$$

where  $\Phi$  is the velocity potential,  $U$ ,  $V$  and  $W$  are contravariant velocity components,  $\rho$  is the density, and  $J$  is the grid Jacobian.

The FPX/FPR codes solve Eq. (3) using an implicit finite-difference scheme, where the time-derivative is replaced by a first-order backward differencing and the spatial-derivatives are replaced by second-order central differencing. The resulting difference equation is approximately factored into three operators  $L_\xi$ ,  $L_\eta$ , and  $L_\zeta$  in  $\xi$ ,  $\eta$  and  $\zeta$  directions, respectively

$$L_\xi L_\eta L_\zeta (\Phi^{n+1} - \Phi^n) = RHS \quad (5)$$

The detail of the scheme is presented in References 6 and 7.

The FPX is the substantially modified version of the FPR code. Both entropy and viscosity corrections are included in the FPX code. The entropy correction potential formulation accounts for the shock produced entropy to enhance physical modeling capabilities for strong shock cases. Either a two-dimensional or a three-dimensional boundary layer model is coupled with the FPX code to account for viscosity effects. In addition, an axial flow capability is added into the FPX code to treat tilt-rotors in forward flight. In addition to the O-H grid topology, an H-H grid topology is added as well. More recently, the Vorticity Embedding (VE) is incorporated into the FPX code to enhance the prediction capability of parallel blade-vortex interactions<sup>11</sup>.

A grid generation package GRGN3 is used to generate O-H mesh around rotor blade. The blade surface is defined by an input file. The far-field boundary of the mesh is set at a fixed number of chords from blade surface. The mesh points are generated between blade surface and far-field boundary. This grid generator is combined into the flow solver FPX recently<sup>12</sup>.

#### 4. Implementation

The coupling of the CDISC design method with the rotor FPX code is the main scope of the present work. Two methods can be used for coupling the CDISC module with the FPX flow analysis code: direct coupling where the CDISC module is treated as a subroutine called by the flow solver; and indirect coupling where a job control language is used. The indirect coupling offers advantages in code maintenance and portability, and the design module does not add to the central memory requirement. In the present work, an indirect coupling is used where a UNIX script file is used to control entire design procedure automatically. User interference during the design processes is not needed.

Information is passed between the CDISC module and the FPX flow solver using blade section geometry file and surface pressure coefficient file. The FPX flow solver with a built-in grid generator<sup>12</sup> is used in this coupling, so that the grid can be re-generated within the flow solver each time when a new blade section geometry file is obtained from the CDISC module. Some modifications on input and output statements to the CDISC code and the FPX code are made as required by the coupling, and thus any type of auxiliary pre- or post-processor codes is not needed. The UNIX script file starts the FPX flow solver to produce an output file containing blade section surface pressure coefficients. This file along with the initial blade section geometry file is then fed into the CDISC design module. The CDISC design module then produces a new geometry file. This new geometry file is used as input for the FPX flow solver. The built-in grid generator generates a new grid and then the flow solver produces a new surface pressure coefficient file. This procedure continues for desired number of cycles as specified in the UNIX script file. Typical cases take 15-30

cycles to get a convergent design.

## 5. Results

As a test of capability of the new package using the CDISC and the FPX codes in rotor section design, several sample design cases are made for a rotor blade. The planform of the blade is shown in Figure 1 along with seven design stations as indicated. The blade has a zero-twist. The first three cases are basic DISC design where target pressure distributions are pre-defined without any constraints. The next two cases are CDISC design where target pressure distributions are automatically generated. The following sub-sections present these results.

### 5.1 Basic DISC Results

In all three basic DISC design cases, initial blade sections are NACA0012 airfoil sections and target pressure distributions are obtained from a known "target" geometry. The new design package is then used to "reproduce" the original "target" configuration. The tip Mach number is set at 0.6288 for the first and second cases, 0.95 for the third case.

In the first case, the "target" geometry is NACA0008 airfoil section. Thirty design cycles are executed to get a convergent (almost convergent at tip-station) design. This case requires around 26 minutes on the Cray-C90 computer with a single processor. The results of this case are presented in Figures 2a-2e. Figures 2a and 2b are design history in terms of blade section geometry and surface pressure distributions, respectively. Figure 2c gives design history of spanwise lifting coefficients, moment coefficients and drag coefficients. A good approximation to the target pressure distributions is achieved after only a few (ten) design cycles (target pressure is given next). Figure 2d gives a comparison of design geometry and target geometry along with the initial geometry, while Figure 2e gives a comparison for surface pressure distributions for four design stations as indicated (although a total of seven stations are designed). The correlation between the final design and target pressure distributions at each station is very good. The new airfoil sections generated compare well with the original "target" geometry.

The second case is very similar to the first case. In this case however, the "target" geometry is an "after-design" NACA0008 airfoil, where a CDISC procedure is first applied to NACA0008 to produce a modified airfoil for reducing drag. The target pressure distribution is the final design pressure during this design process. The results of this case are presented in Figures 3a-3e. Figures 3a-3c are design history. Figures 3d and 3e are comparison of design and target. A good agreement between design and target is obtained again.

In the third case, the "target" geometry and target pressure are provided from a

CDISC design case applied to MDHC HH02 and NACA64A006 airfoil sections. It is expected that a large number of design cycles is needed for this case to get a convergent design due to a substantial difference between the initial geometry and the “target” geometry, particularly at tip station. As a consequence, 300 design cycles are executed for this case to examine the nature of convergence. The results of this case are presented in Figures 4a-4g. Figures 4a and 4b are design history in terms of airfoil section geometry and surface pressure distributions, respectively. Figure 4c gives design history of spanwise lifting coefficients, moment coefficients and drag coefficients. It is seen that the solution is convergent between design cycles 150 and 200 for Stations 1, 3 and 5, and almost convergent at design cycle 300 at Station 7 (the tip station). Figures 4d gives a comparison of final design geometry and target geometry along with the initial geometry, while Figure 4e gives a comparison for surface pressure distributions for the four design stations. The correlation between the final design and target pressure distributions at Stations 5 and 7 is very good. However, some discrepancies exist for Stations 1 and 3. Same is true for the comparison of geometry. Figures 4f and 4g then made another comparison of target with design where design geometry and pressure are obtained at design cycle 50 for Stations 1, 3 and 5. It is now noted that the agreement between design and target is better than that of Figures 4d and 4e for Stations 1 and 3, particularly for Station 1.

## 5.2 CDISC Results

With the Constrained DISC approach, the emphasis is shifted to meeting the constraints where target pressure is generated automatically within the design module. In the next sample cases, two constraints are imposed: one to fix the original spanload distribution, and other one to reduce drag using the Modified Uniform Distribution (MUD) of chordwise loading constraint option. A MUD value of 0.2 is used according to Campbell<sup>5</sup> to obtain a best result in reducing drag. The tip Mach number is set at 0.95. In both cases, 15 design cycles are executed.

Figures 5a-5c are the results of the first CDISC sample design case, where initial blade sections are NACA0012 sections. Figures 5a and 5b give the history of design for blade section geometry and surface pressure distributions, respectively. Figure 5c presents a spanwise lifting coefficient, moment coefficient, drag coefficient and maximum local Mach number distributions. It is seen that the design reduces the negative lifting force, pitching moment and drag force. By examining the drag coefficients, it is found that the drag is reduced by 12.5% at Station 3 and 7.5% at Station 5 through the CDISC design. The maximum local Mach numbers are unchanged during the design process.

Figures 6a-6c are the results of the second CDISC sample design case, where initial blade sections are MDHC HH02 airfoil for Stations 1 through 5, and NACA64A006 airfoil for Stations 6 and 7. Figures 6a and 6b give the history of design for blade section geometry and surface pressure distributions, respectively. Figure 6c presents a spanwise lifting

coefficient, moment coefficient, drag coefficient and shock Mach number distributions. By examining the drag coefficients, it is found that the drag is reduced by 12.7% at Station 1, 9.6% at Station 3, 25.6% at Station 5 and 12.5% at Station 7 through the redistribution of the loading and smoothing. Shock is also eliminated through the design as indicated, in the figure, by zero-shock Mach number along the span.

## 6. Conclusions

A rotor section aerodynamic design package is developed by coupling the CDISC design method with the FPX rotor CFD code. The coupling between the CDISC design and the FPX flow analysis is fully automated using a UNIX script file to control job flow. Five sample design cases are presented for both basic DISC and Constrained DISC design for a zero-twist blade in hovering motion. The results indicate that the CDISC method is a robust and efficient design method when used in rotor section design coupled with the FPX code.

These sample cases demonstrate that the target pressure can be achieved even when the initial geometry is not "close" to the "target" geometry. A constrained DISC design case demonstrates a shock-free design using MUD method, where drag is significantly reduced. Actual computational effort depends on the complexity of the target pressure distributions and the difference between the initial and "target" geometry. A typical design case with 30 design cycles for designing 7 stations requires around 26 minutes CPU time on the Cray-C90 computer with a single processor. Presently, all sample design cases are made to a zero-twist blade without in-flow angles for either symmetric or cambered airfoil section design. The further work is needed in extending the current design package into high-lifting flows with large twist and in-flow angles.

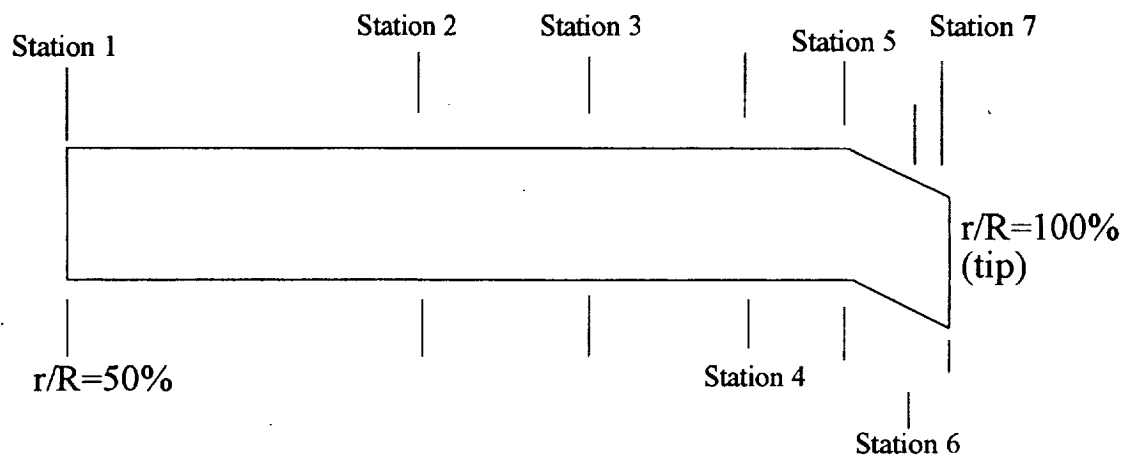


Figure 1. The rotor blade planform.

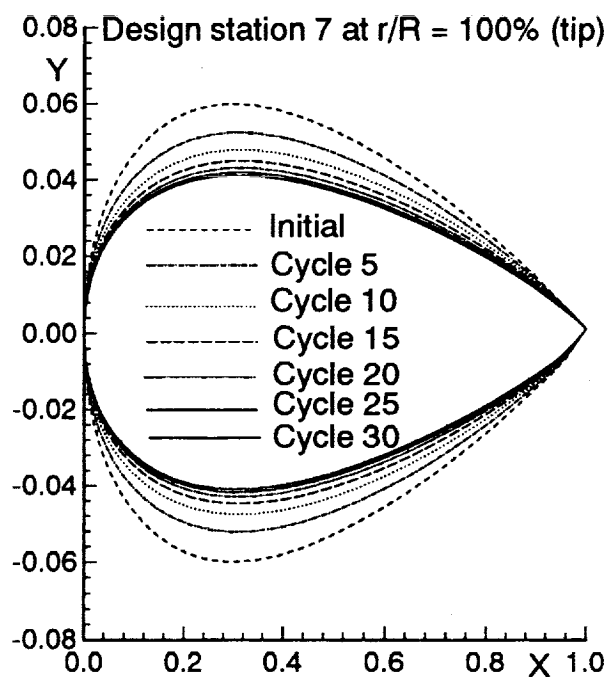
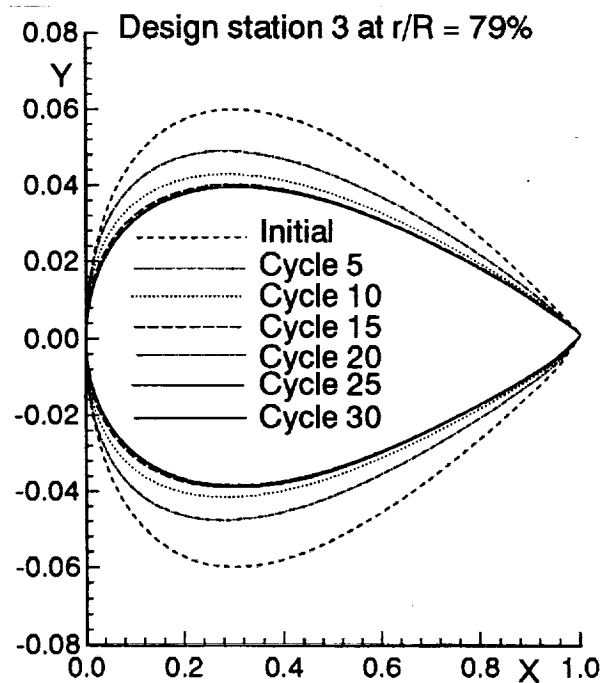
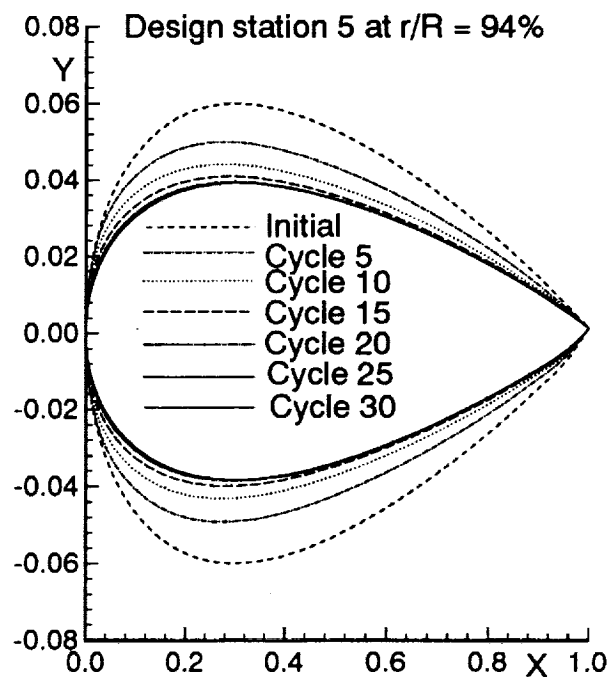
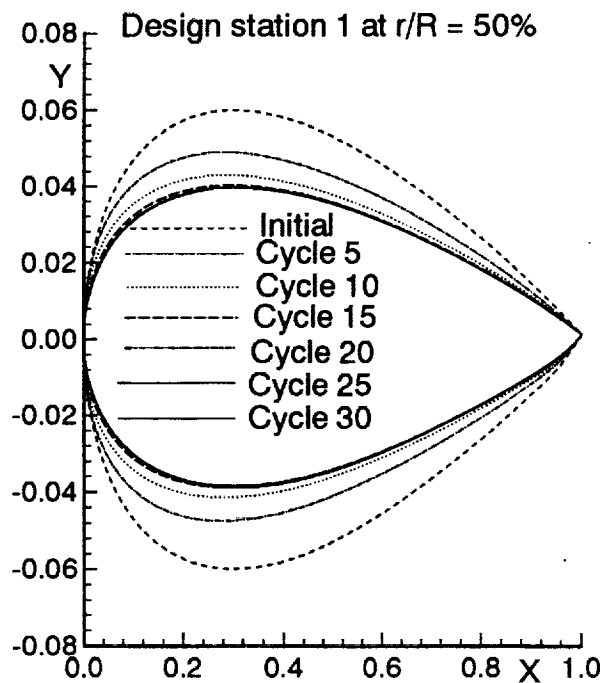


Figure 2a. Design history of blade section geometry for basic DISC design case 1,  $M_{tip} = 0.6288$ .



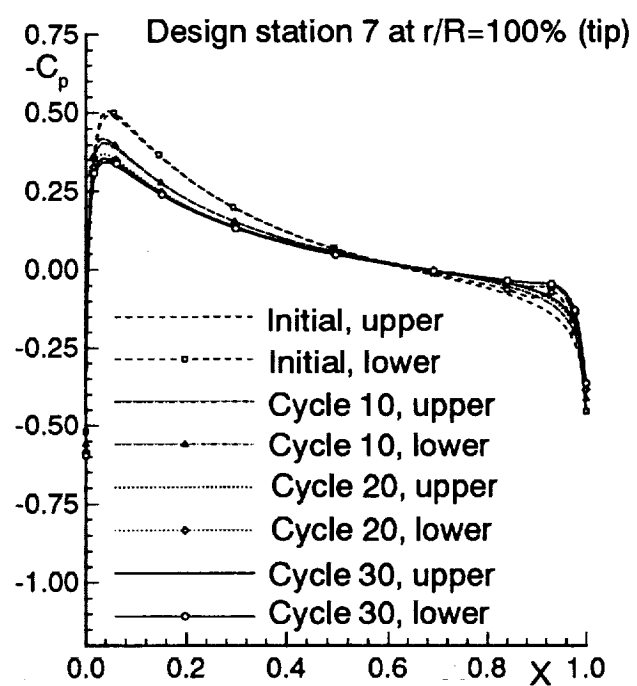
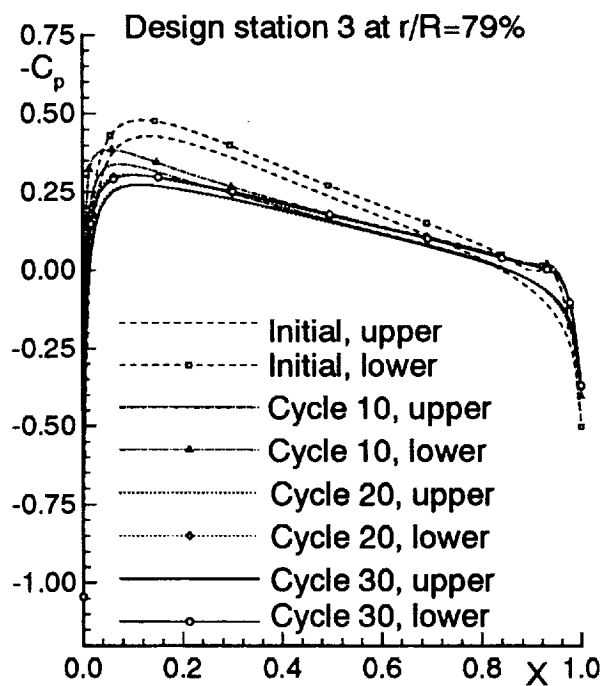
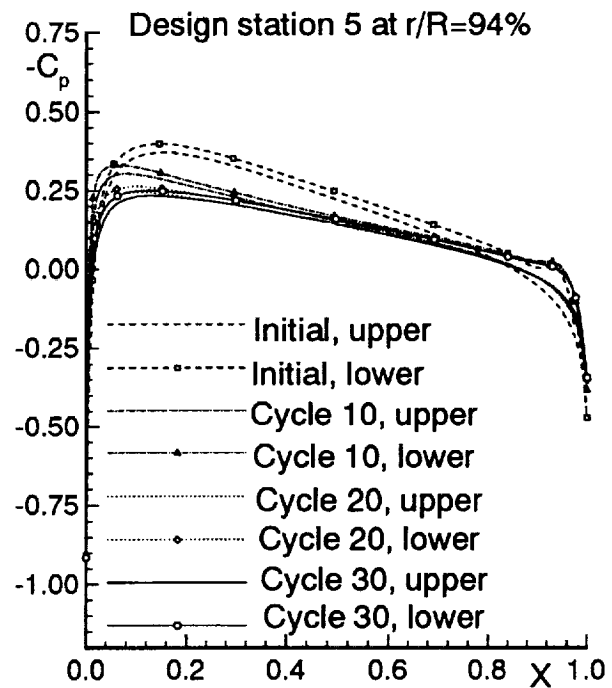
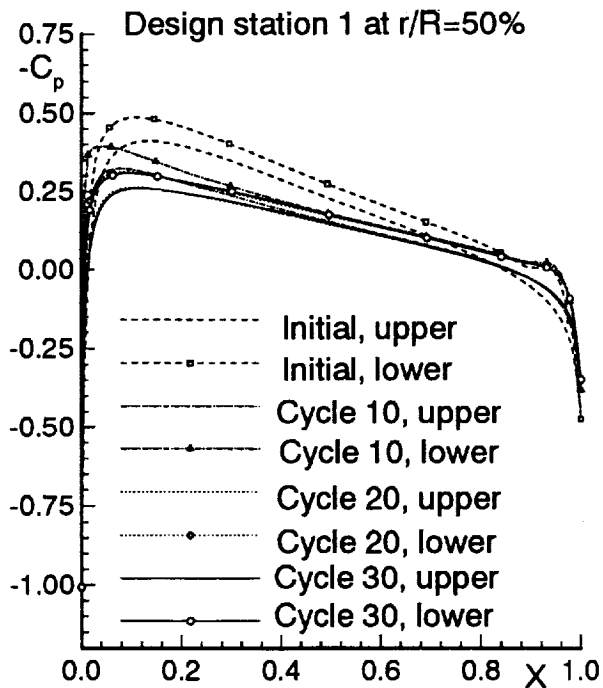


Figure 2b. Design history of surface pressure distributions for basic DISC design case 1,  $M_{tip} = 0.6288$ .

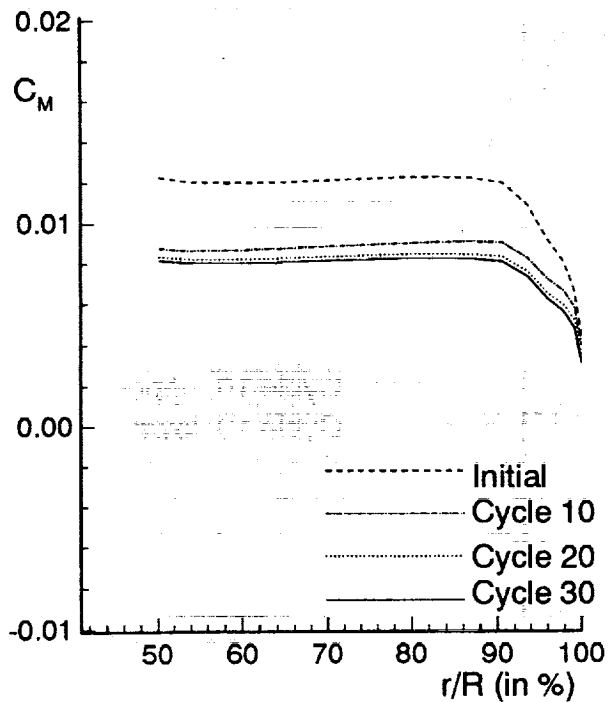
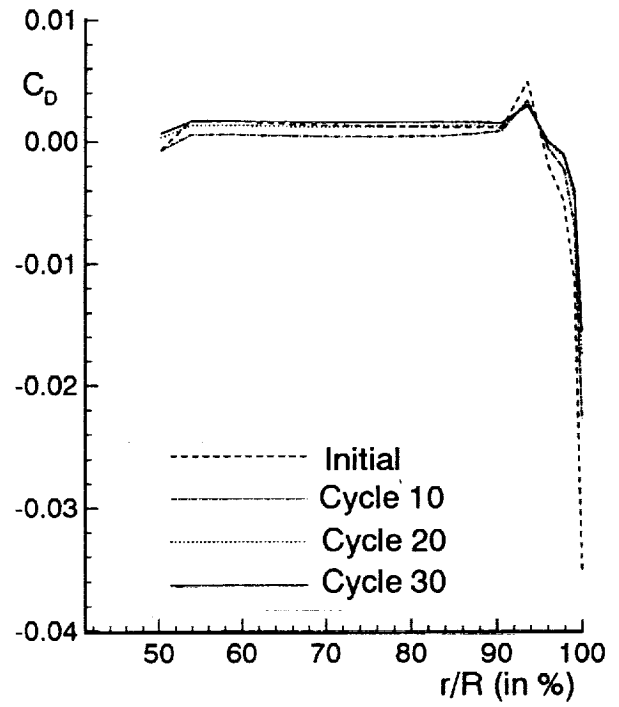
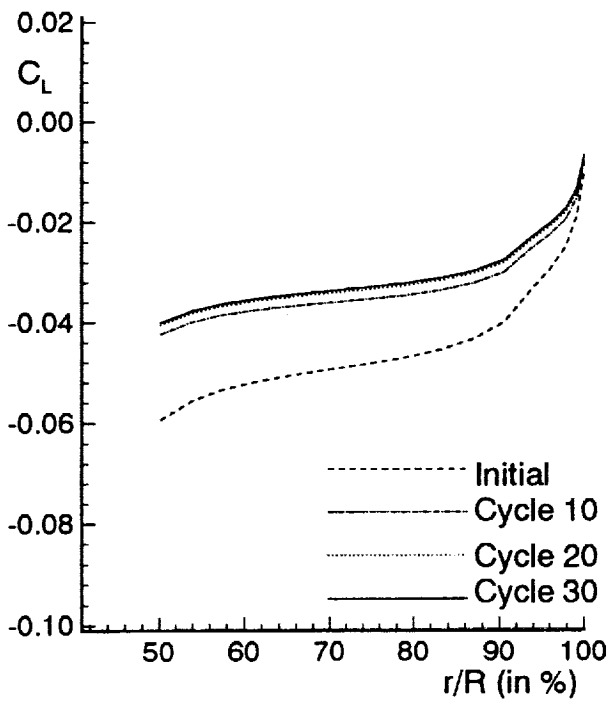


Figure 2c. Design history of spanwise lifting ( $C_L$ ), moment ( $C_M$ ) and drag ( $C_D$ ) coefficients for basic DISC design case 1,  $M_{tip} = 0.6288$ .

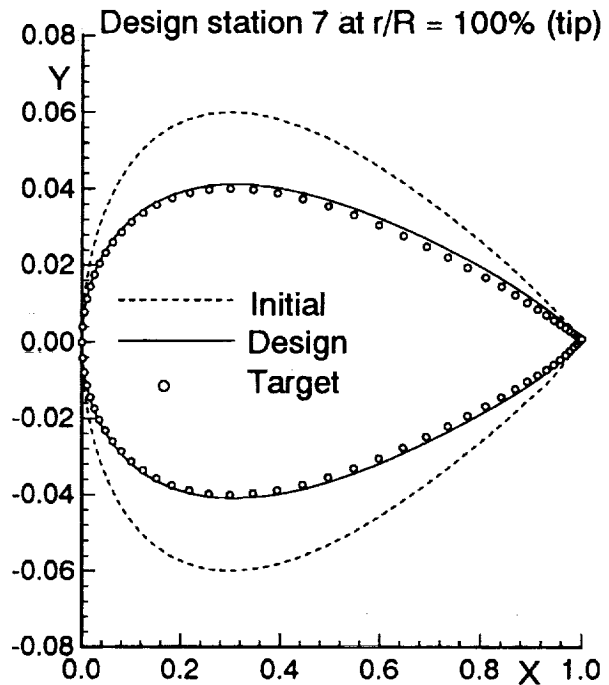
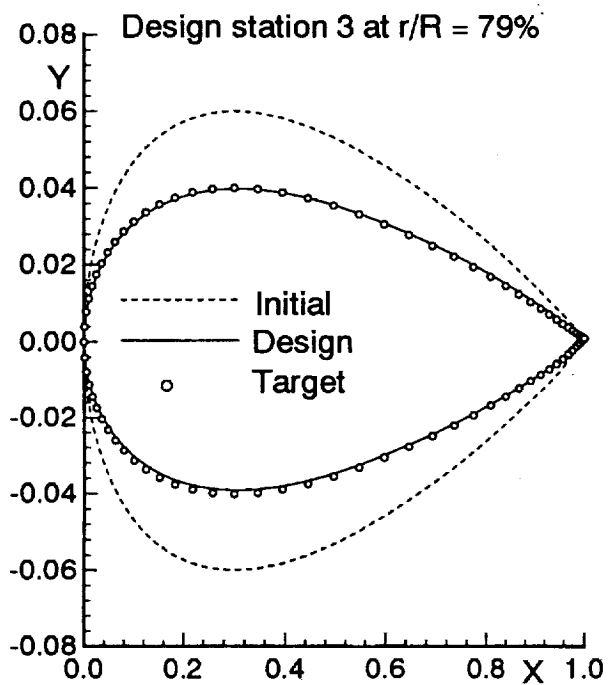
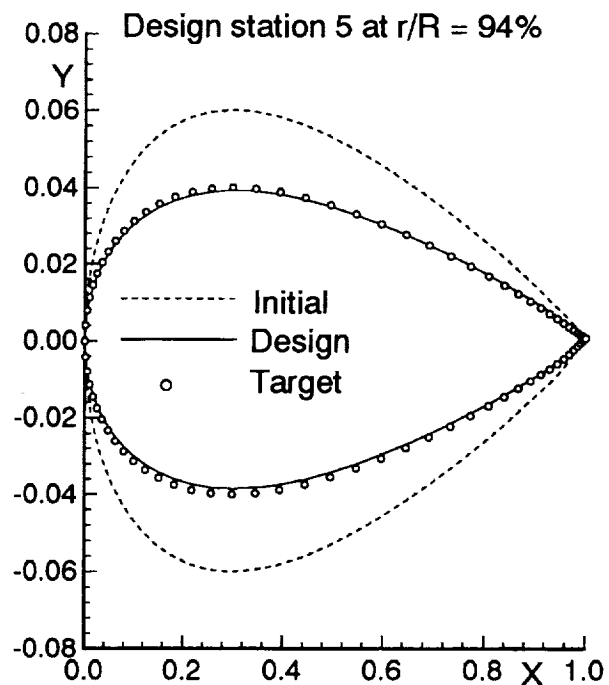
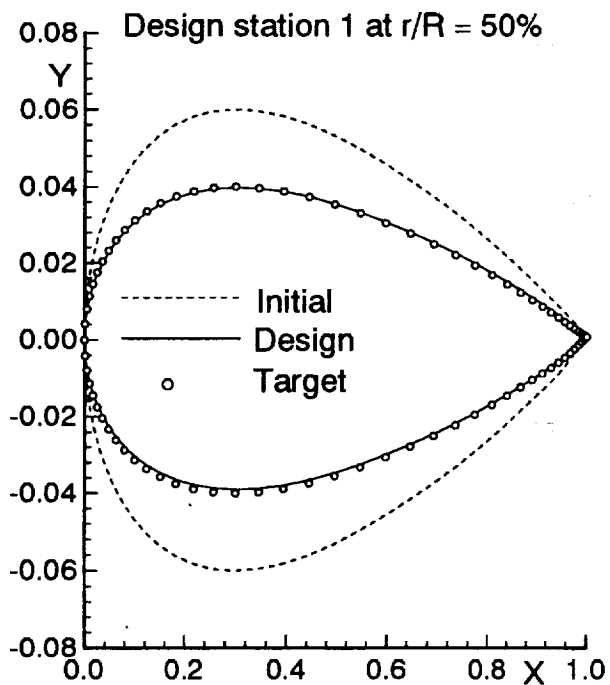


Figure 2d. Comparison of blade section geometry for basic DISC design case 1,  $M_{tip} = 0.6288$ .

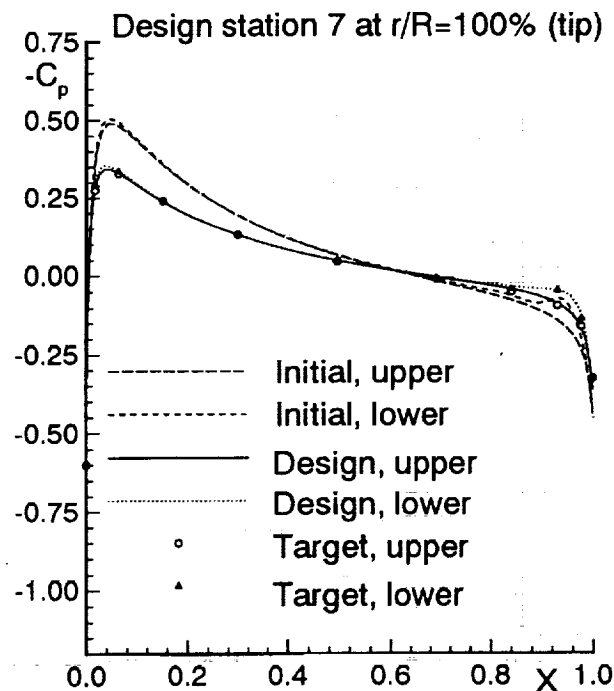
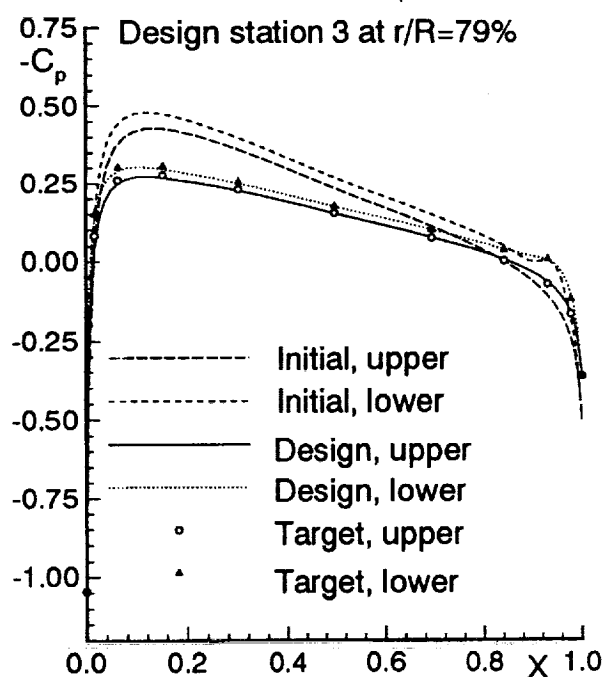
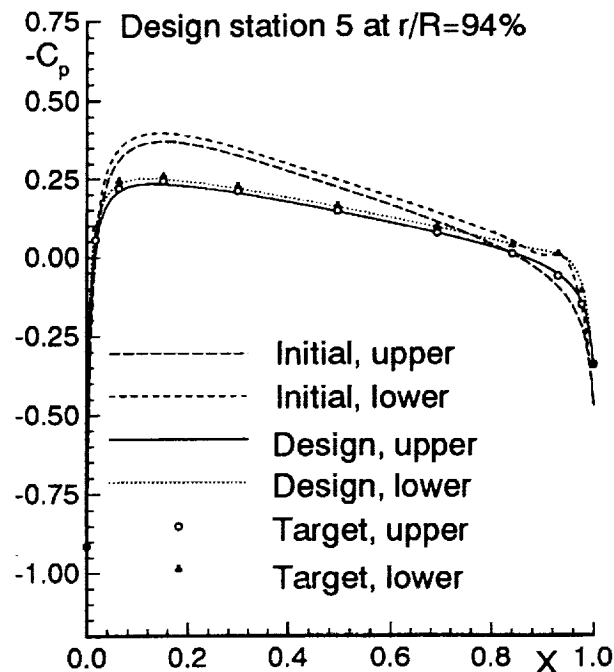
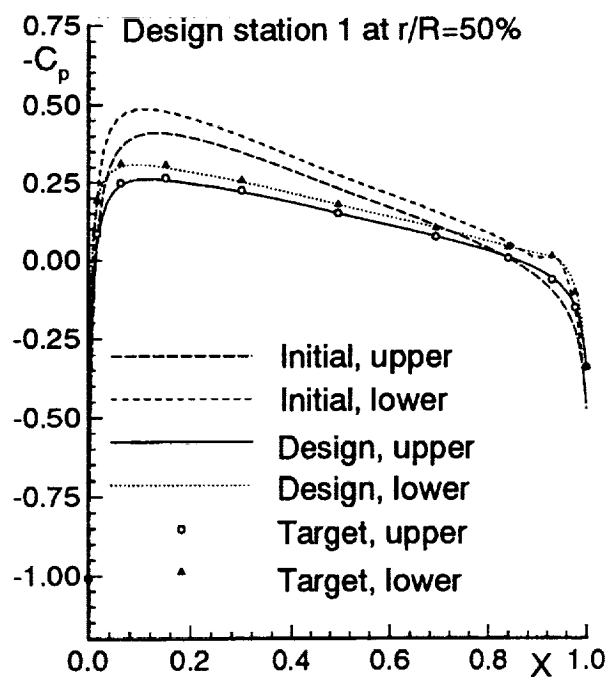


Figure 2e. Comparison of surface pressure distributions for basic DISC design case 1,  $M_{tip} = 0.6288$ .

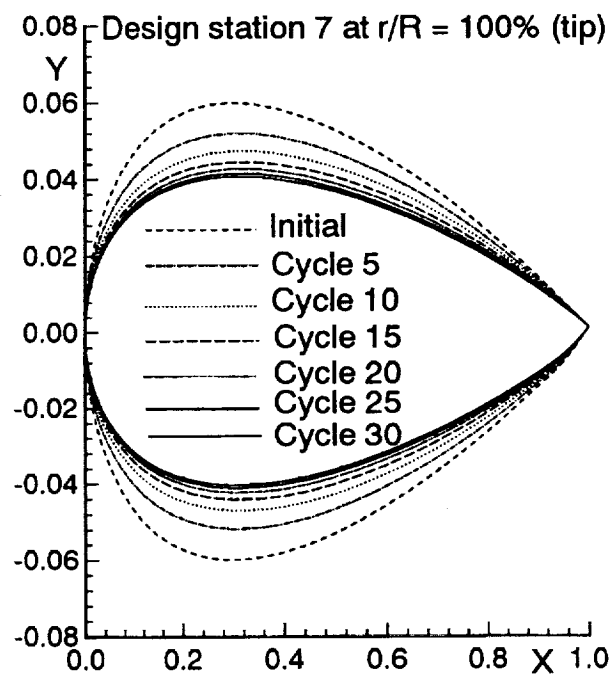
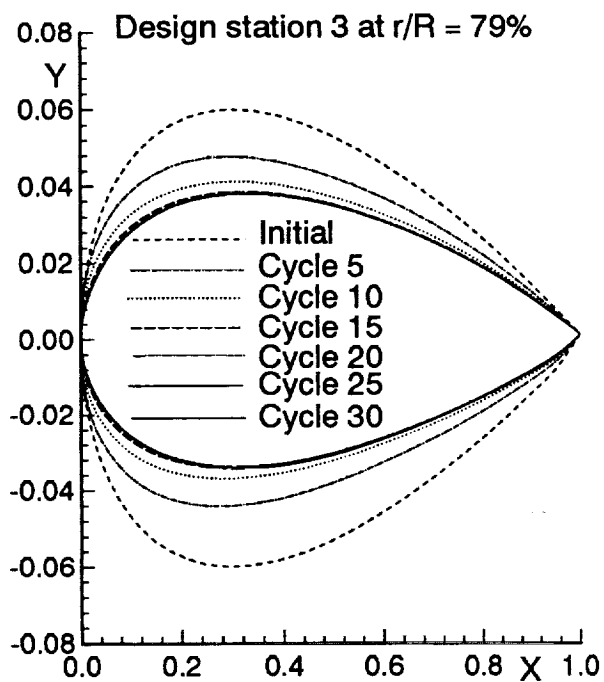
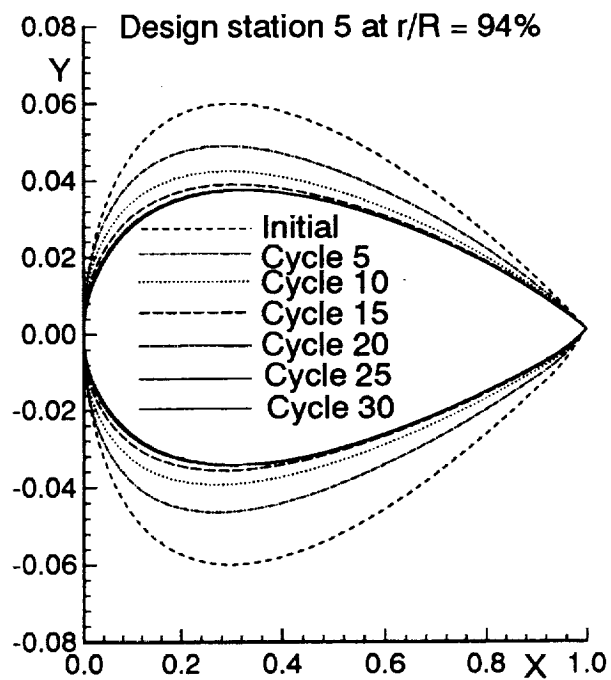
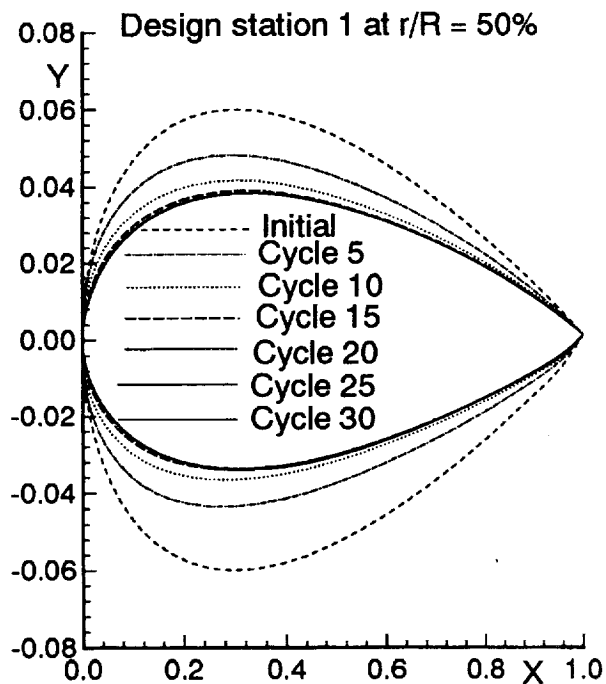


Figure 3a. Design history of blade section geometry for basic DISC design case 2,  $M_{tip} = 0.6288$ .

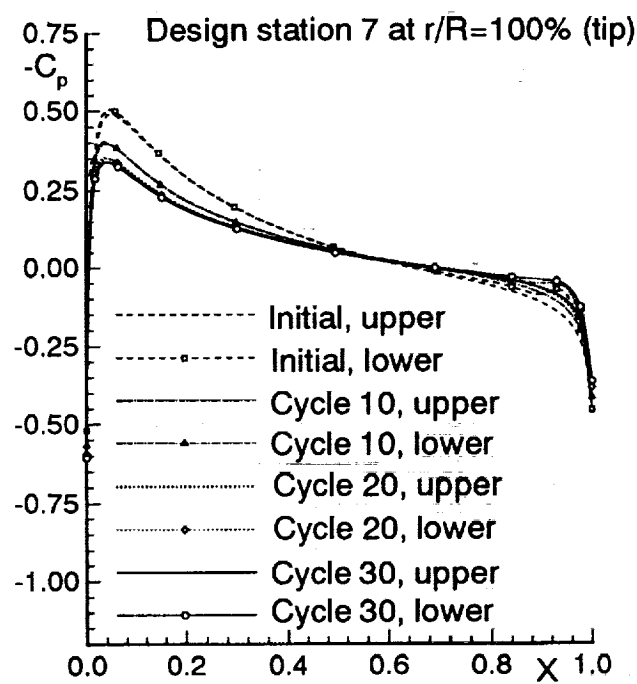
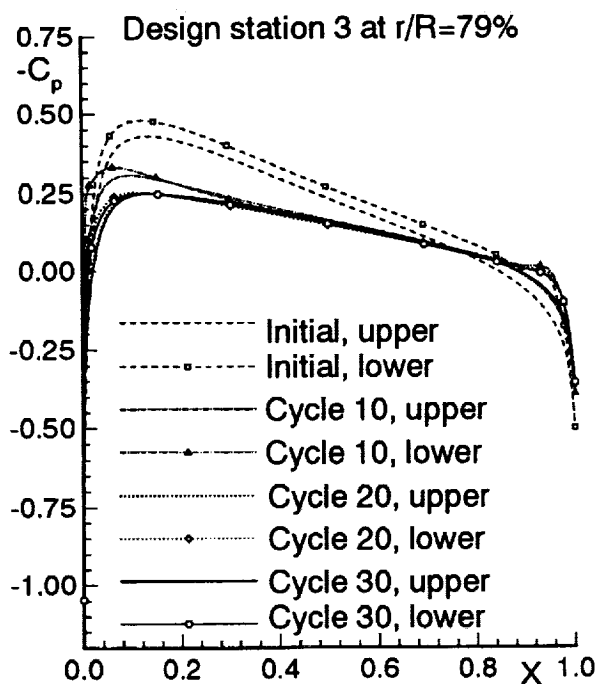
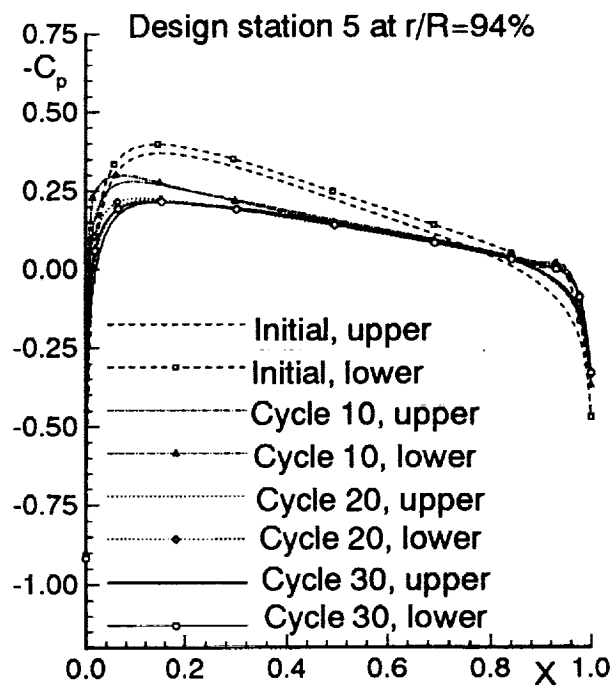
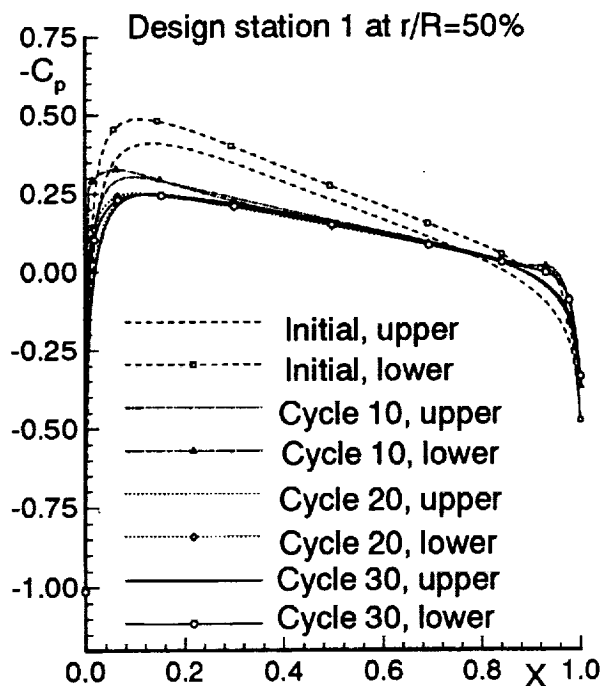


Figure 3b. Design history of surface pressure distributions for basic DISC design case 2,  $M_{tip} = 0.6288$ .

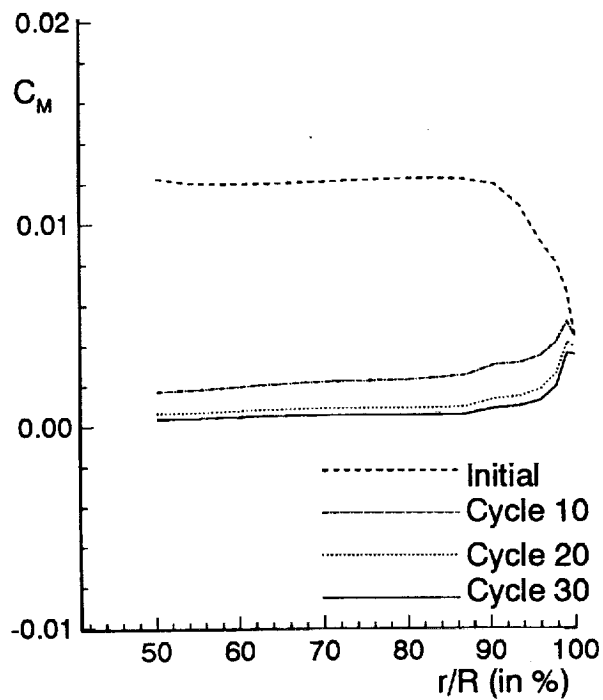
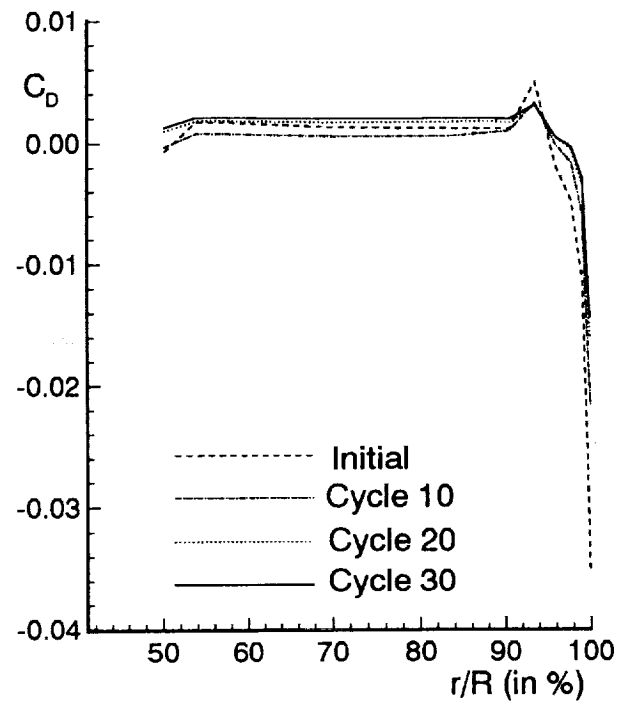
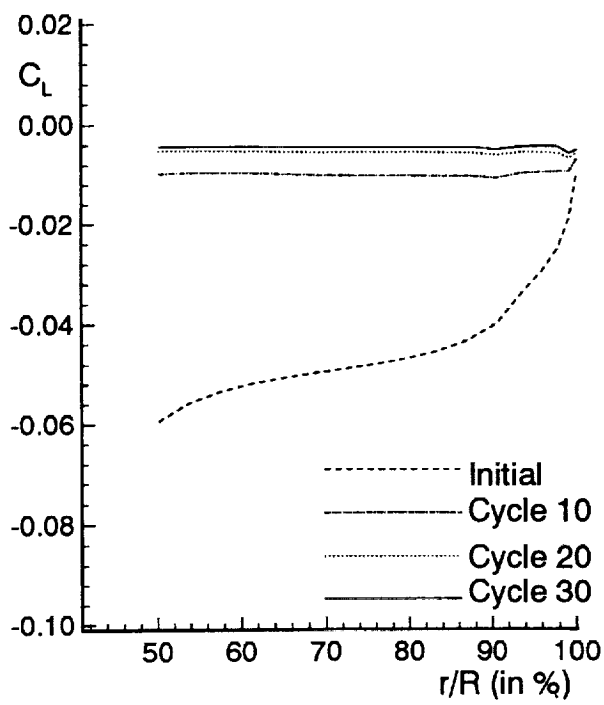


Figure 3c. Design history of spanwise lifting ( $C_L$ ), moment ( $C_M$ ) and drag ( $C_D$ ) coefficients for basic DISC design case 2,  $M_{tip} = 0.6288$ .

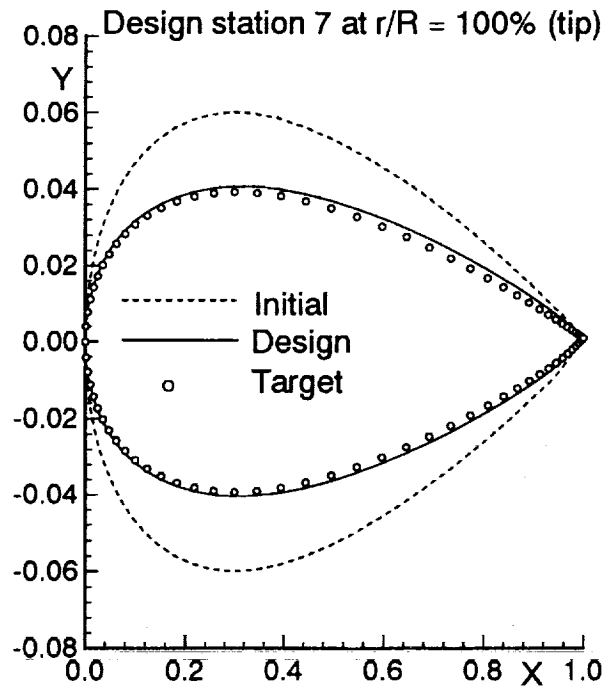
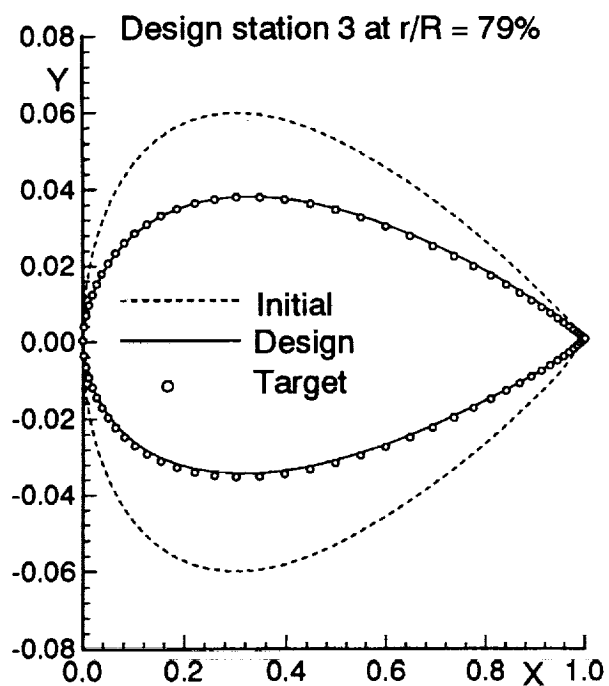
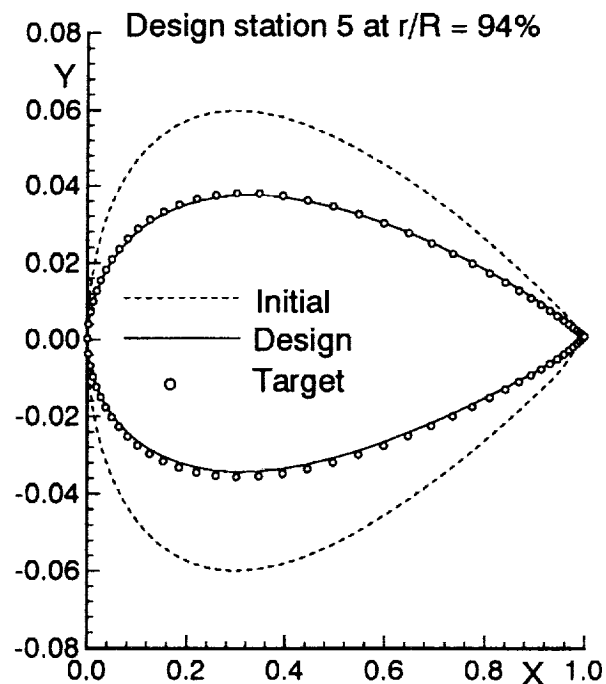
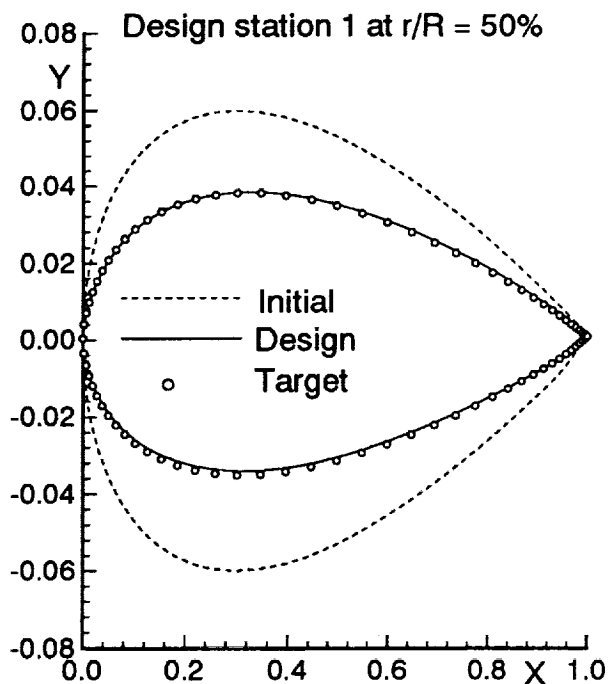


Figure 3d. Comparison of blade section geometry  
for basic DISC design case 2,  $M_{tip} = 0.6288$ .



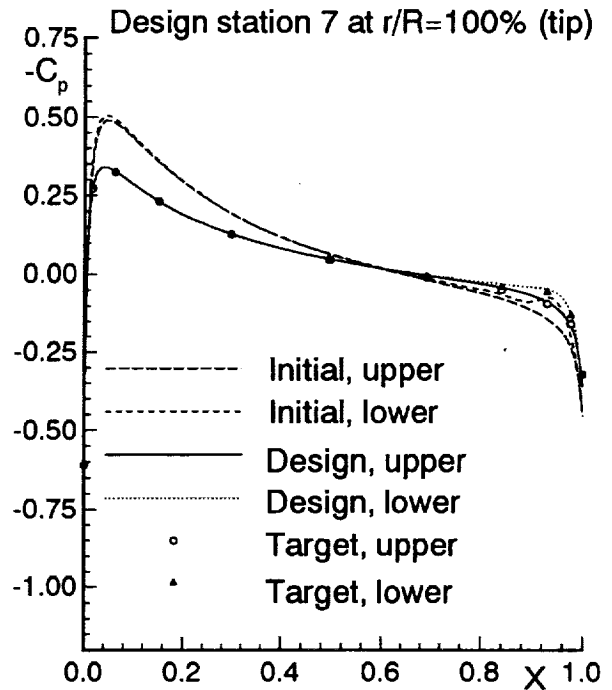
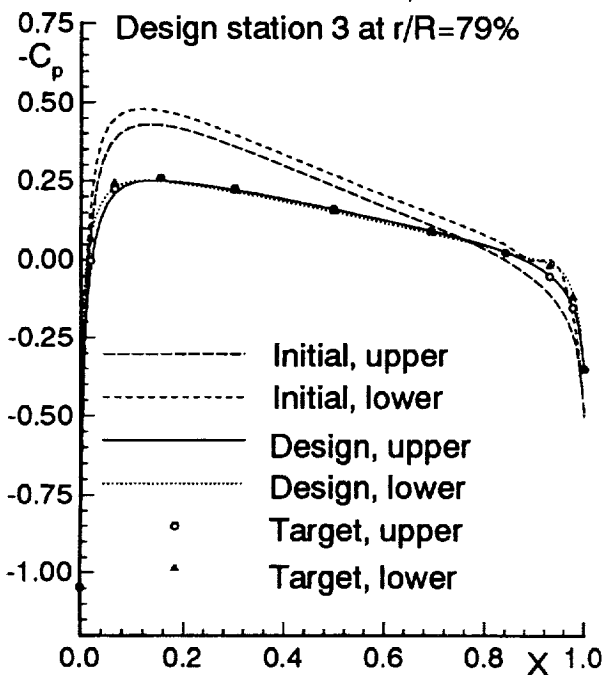
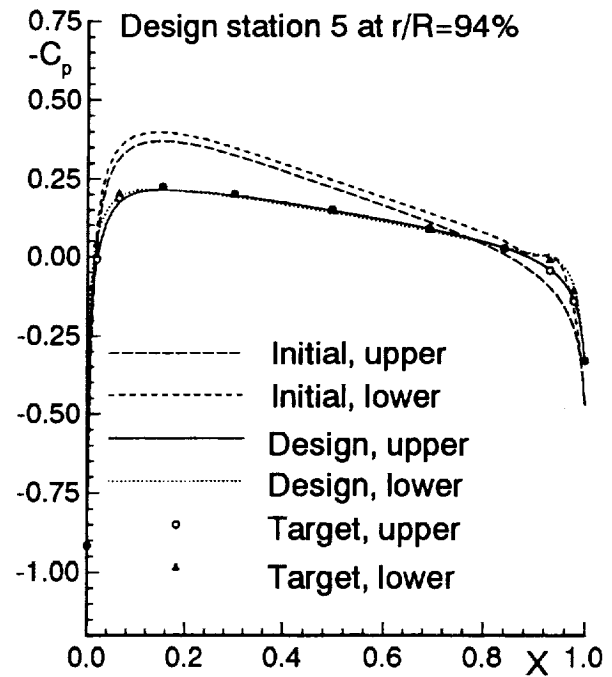
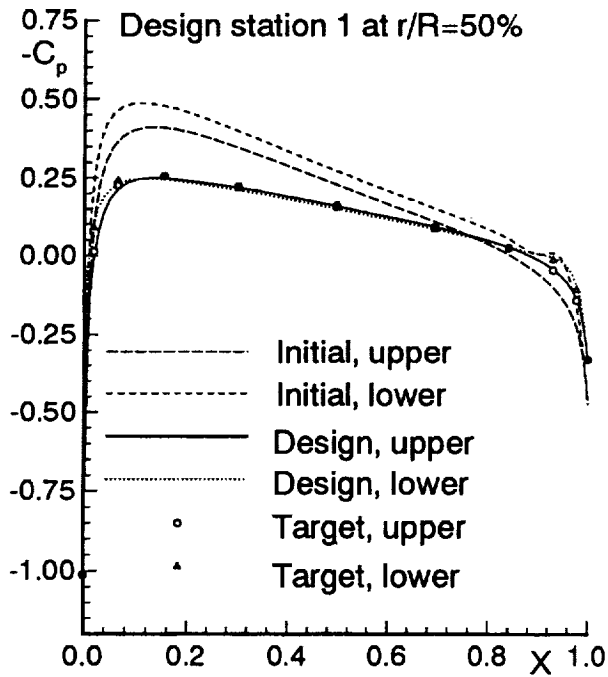


Figure 3e. Comparison of surface pressure distributions for basic DISC design case 2,  $M_{tip} = 0.6288$ .

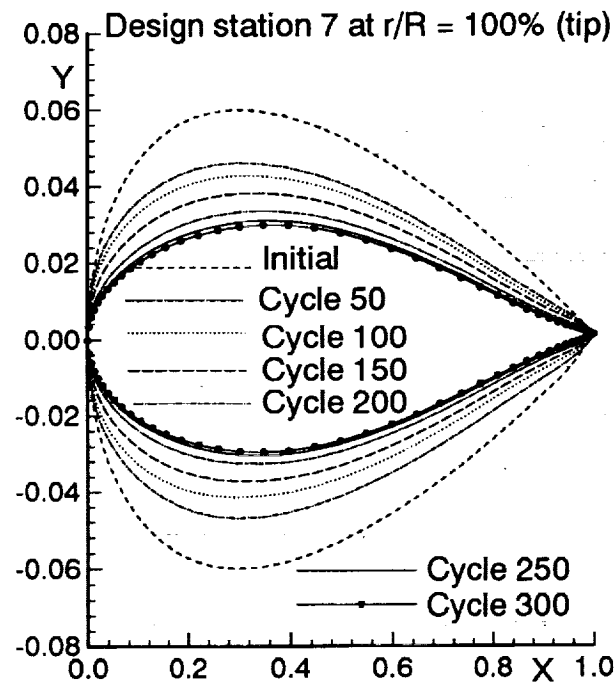
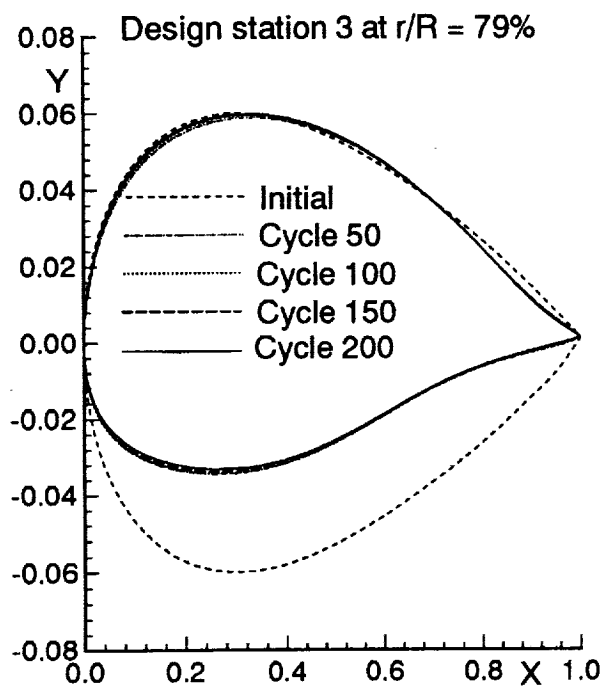
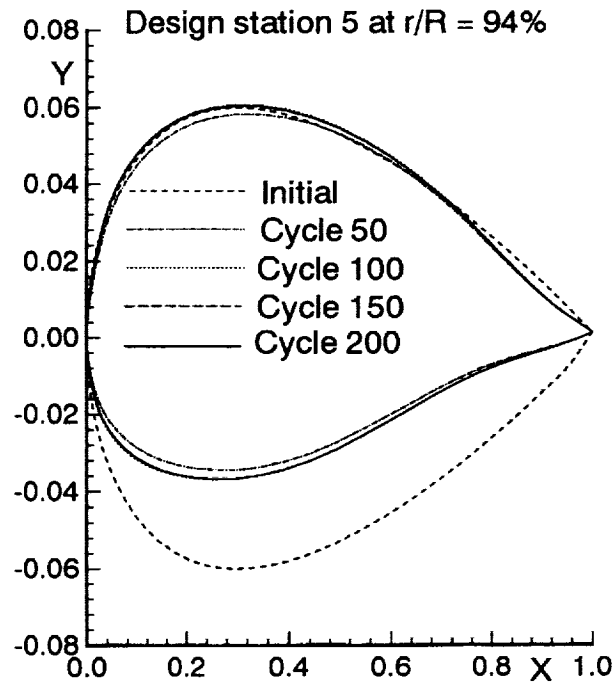
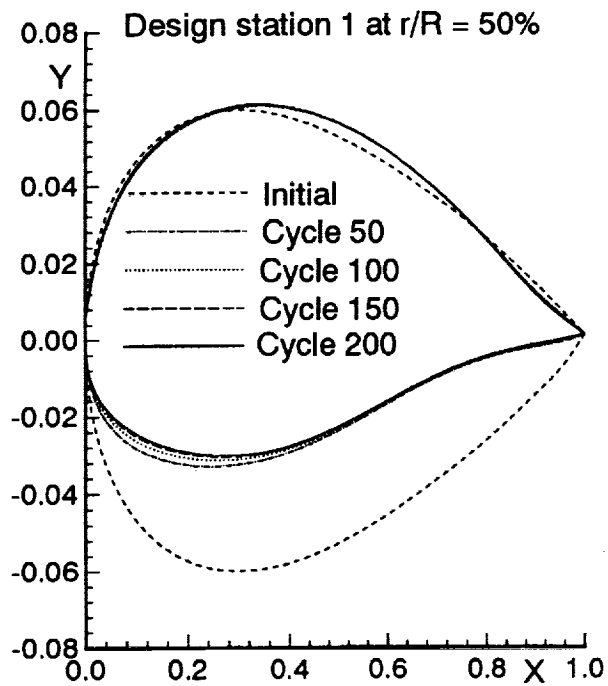


Figure 4a. Design history of blade section geometry for basic DISC design case 3,  $M_{tip} = 0.95$ .

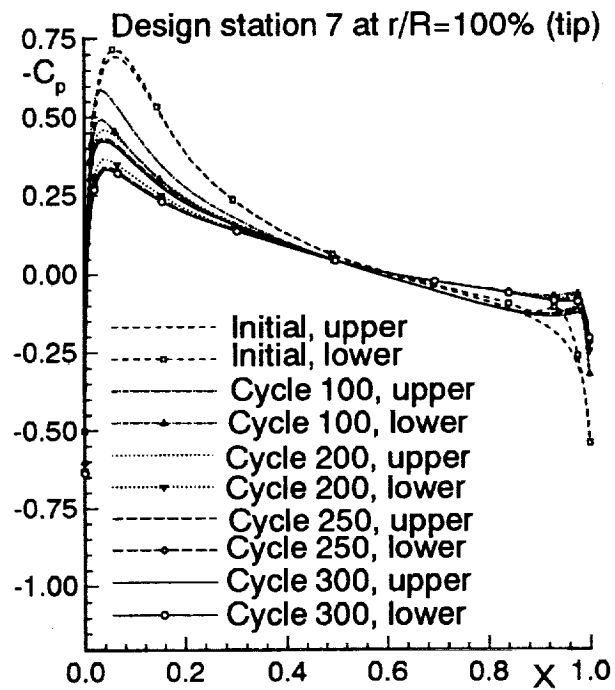
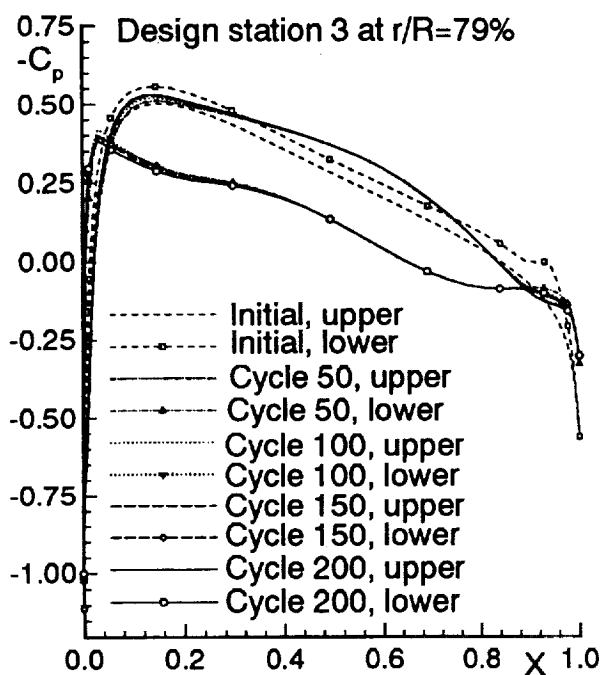
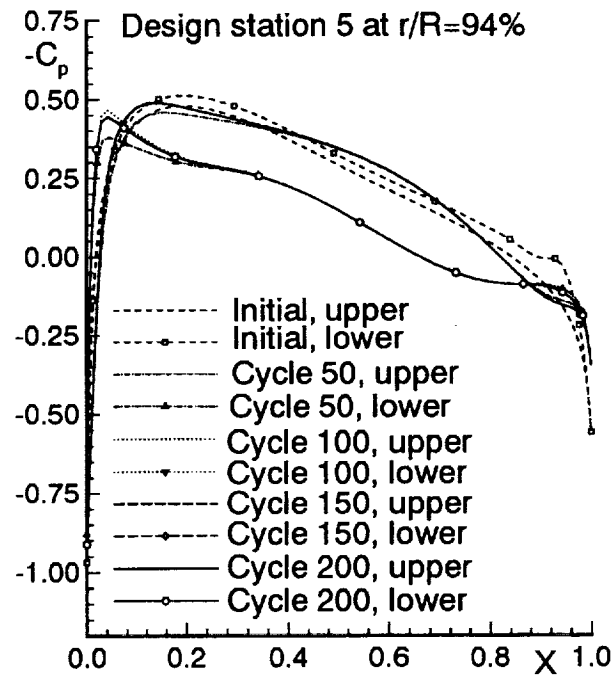
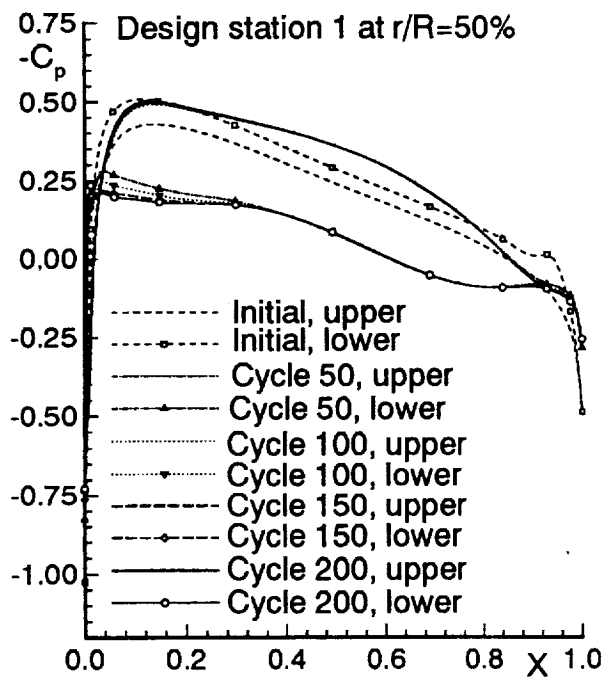


Figure 4b. Design history of surface pressure distributions for basic DISC design case 3,  $M_{tip} = 0.95$ .

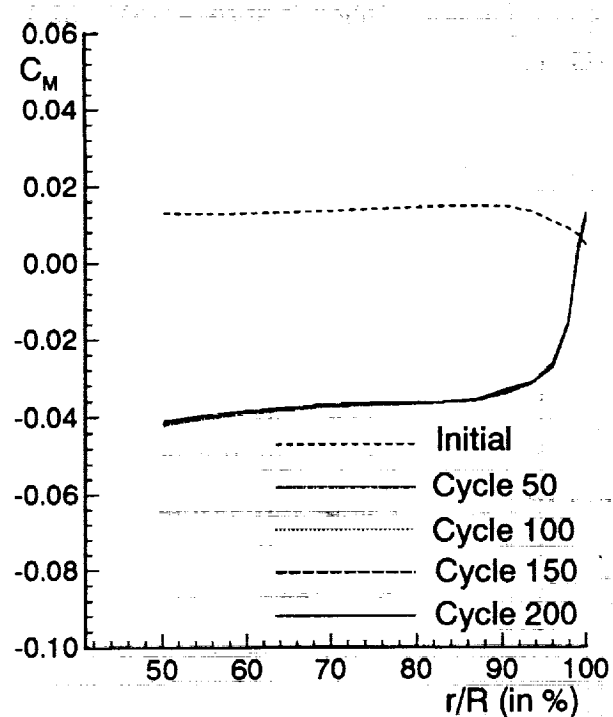
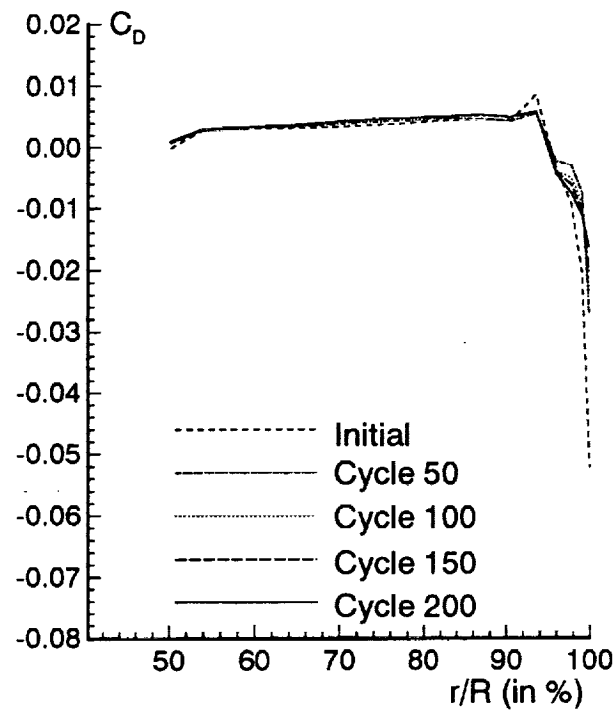
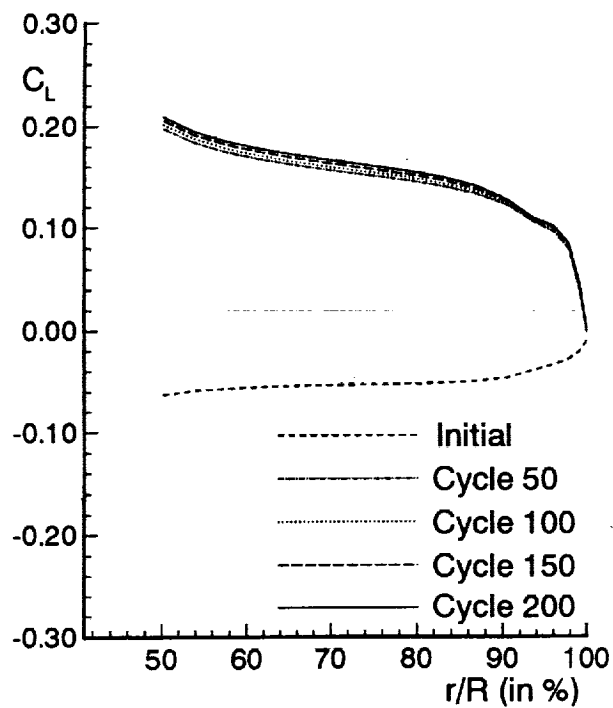


Figure 4c. Design history of spanwise lifting ( $C_L$ ), moment ( $C_M$ ) and drag ( $C_D$ ) coefficients for basic DISC design case 3,  $M_{tip} = 0.95$ .

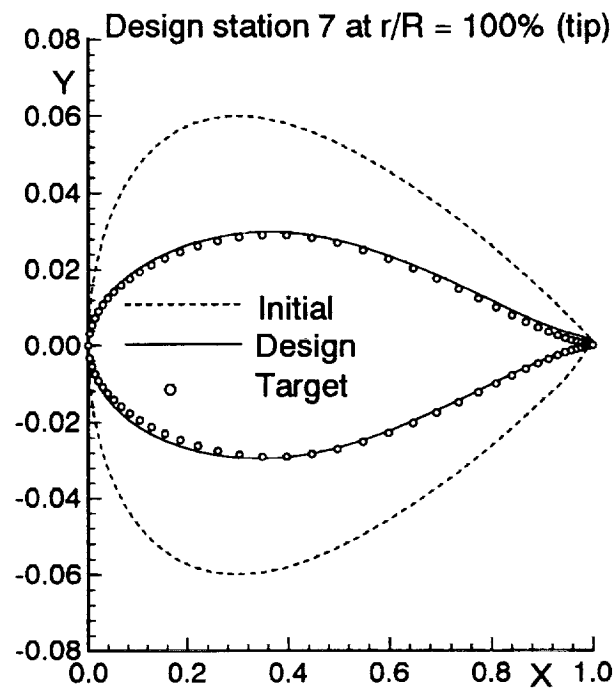
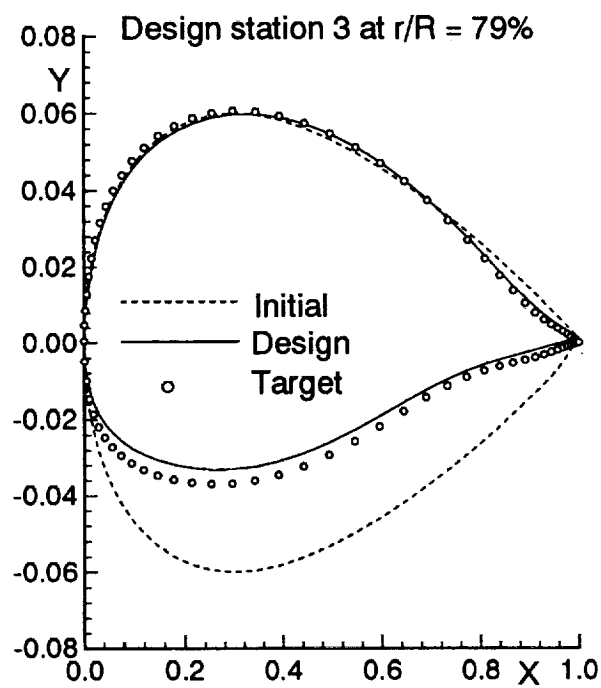
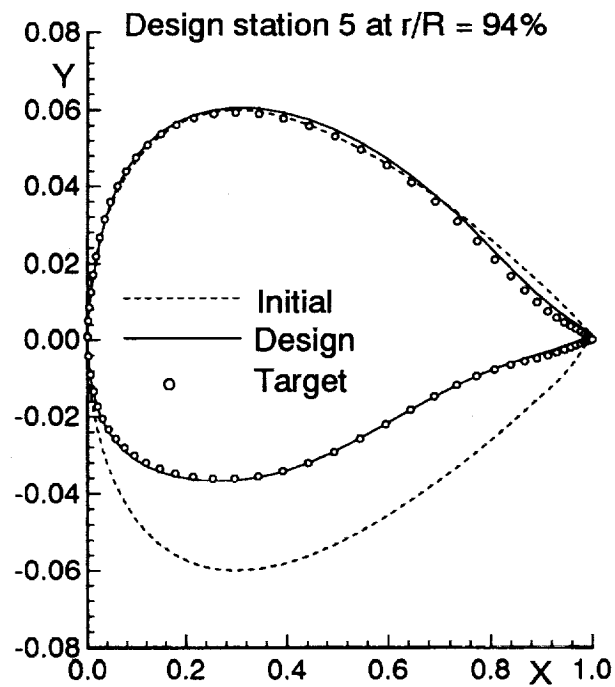
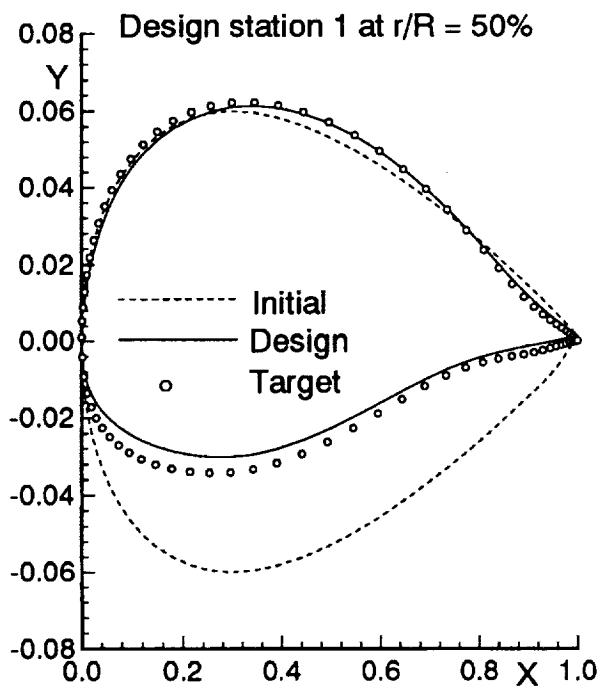


Figure 4d. Comparison of blade section geometry for basic DISC design case 3,  $M_{tip} = 0.95$ , where final design is used.

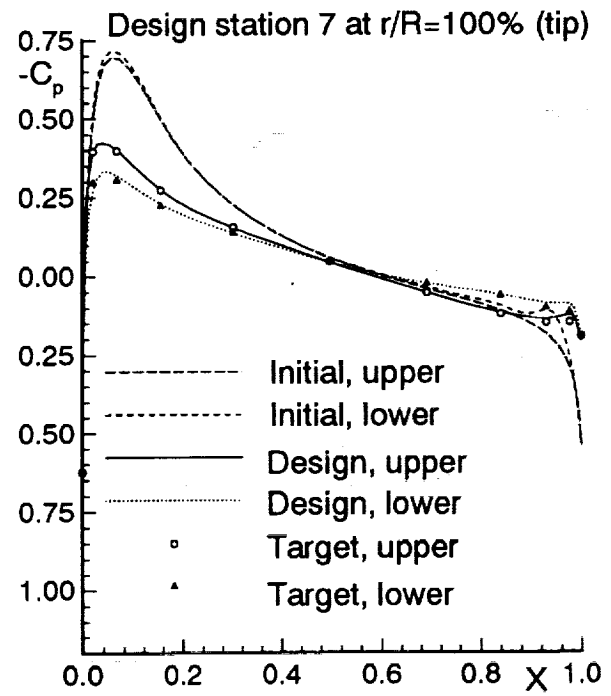
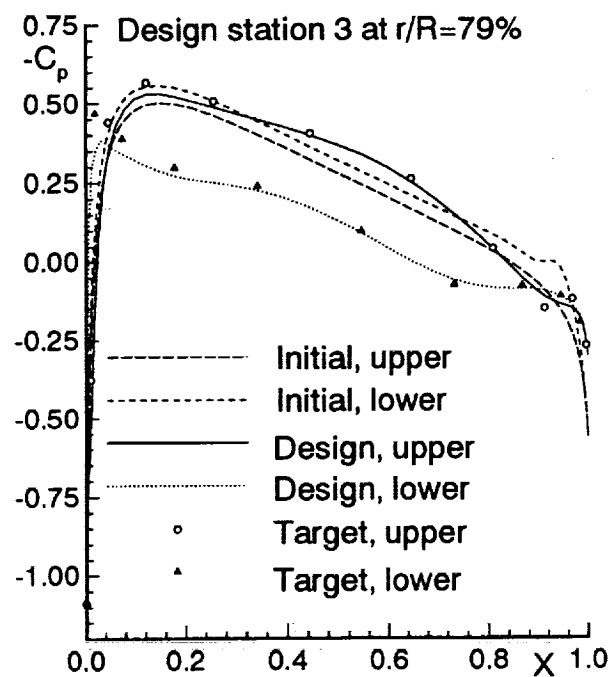
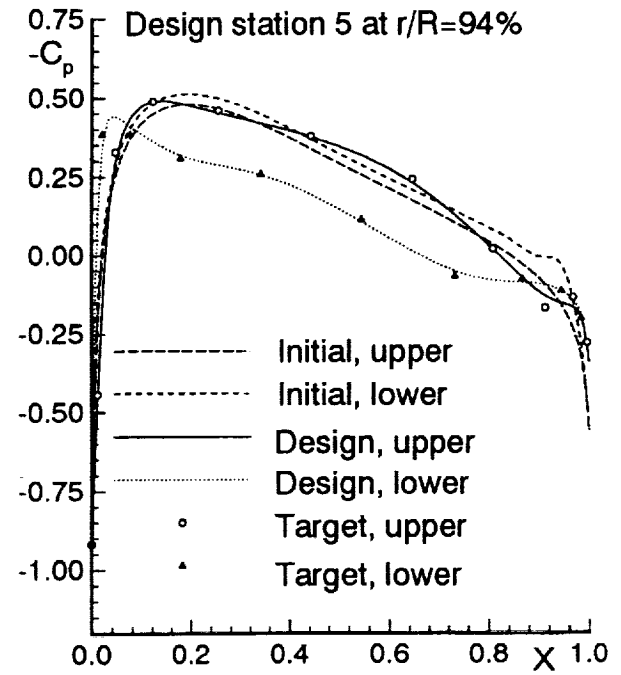
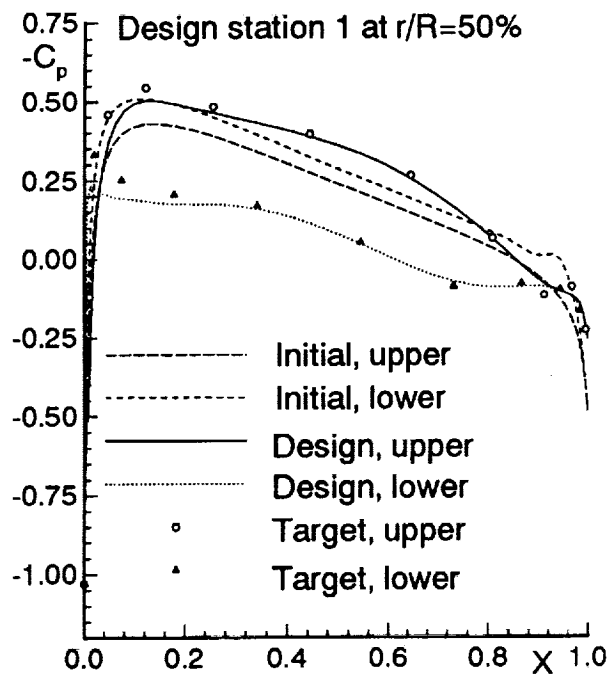


Figure 4e. Comparison of surface pressure distributions for basic DISC design case 3,  $M_{tip} = 0.95$ , where final design is used.

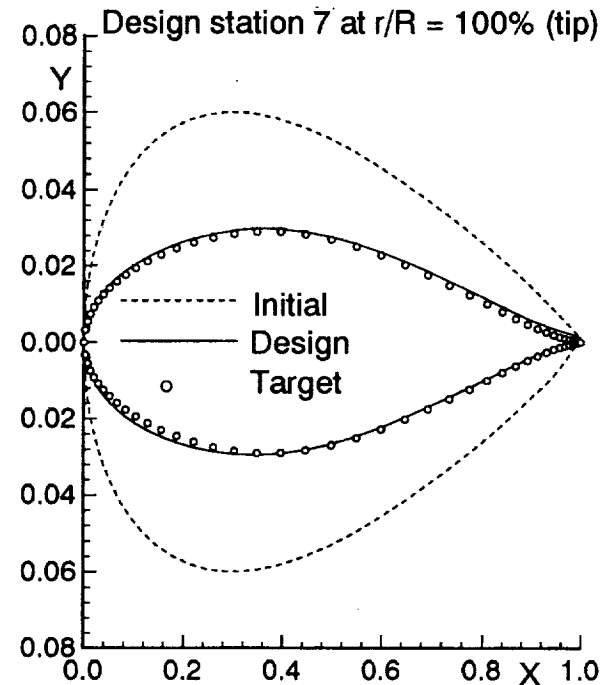
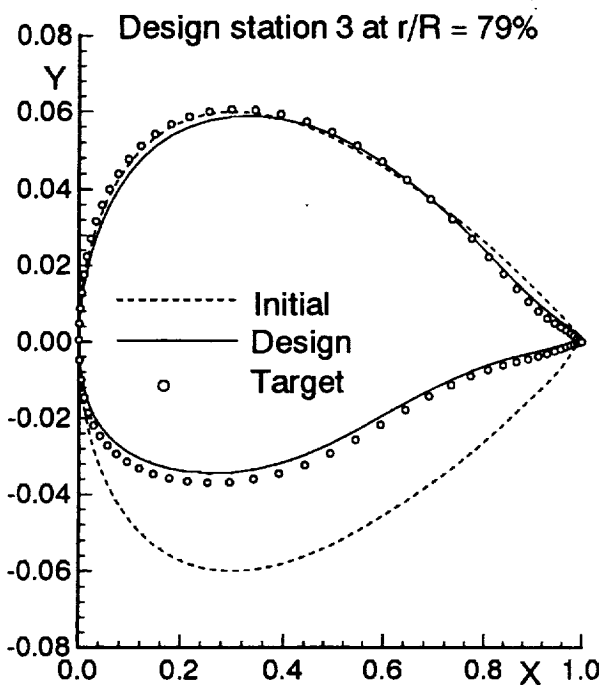
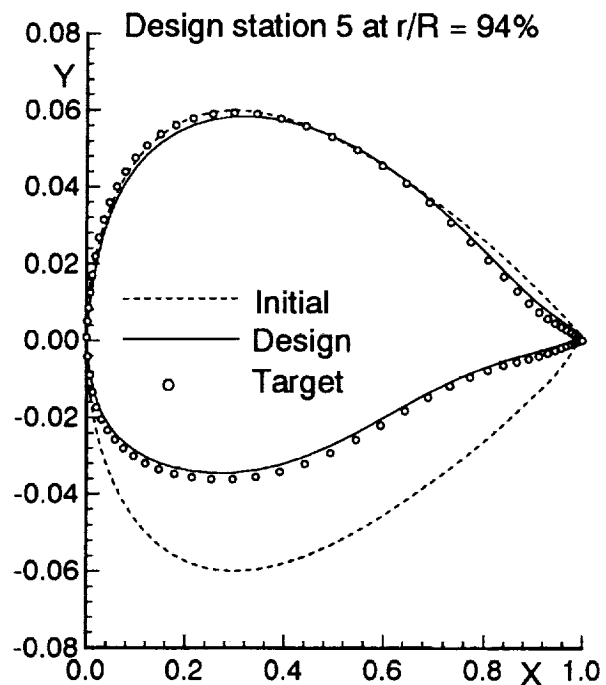
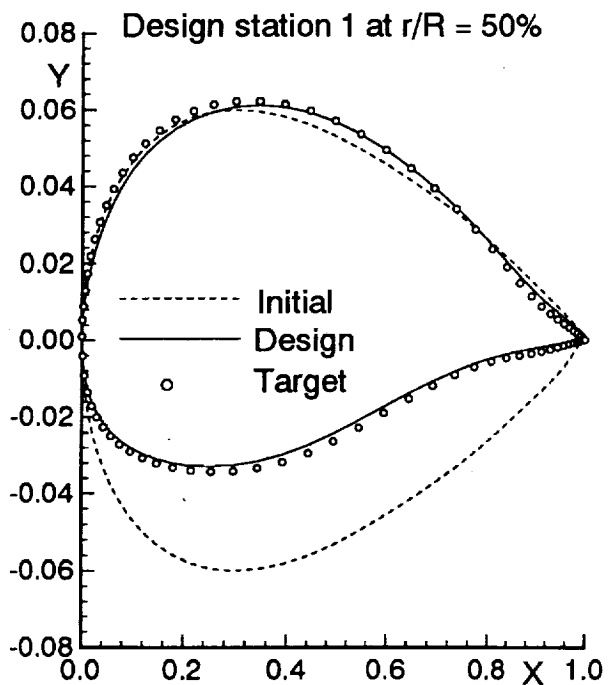


Figure 4f. Comparison of blade section geometry for basic DISC design case 3,  $M_{tip} = 0.95$ , where the design at cycle 50 is used.

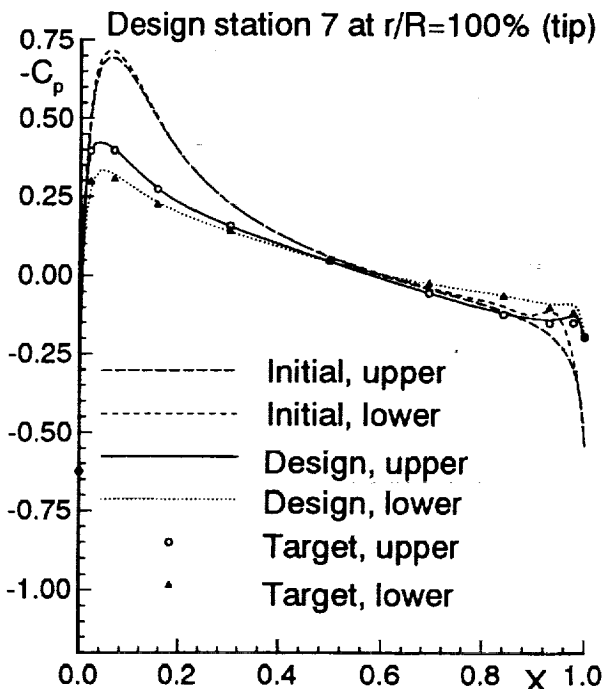
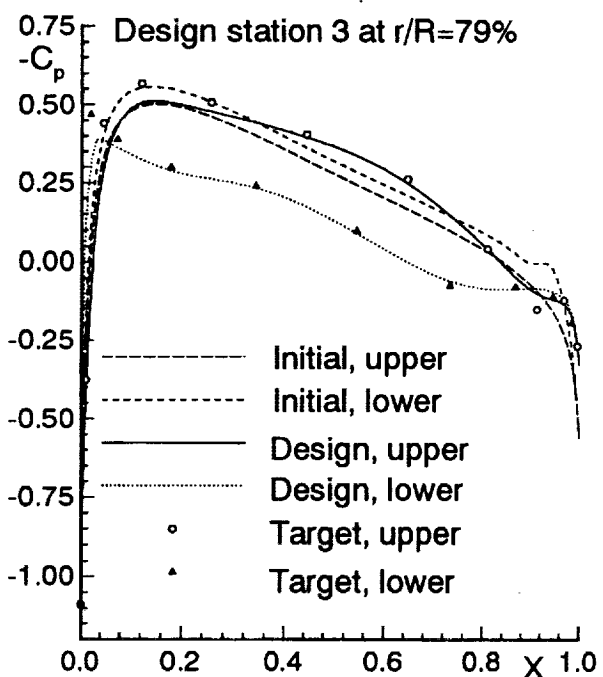
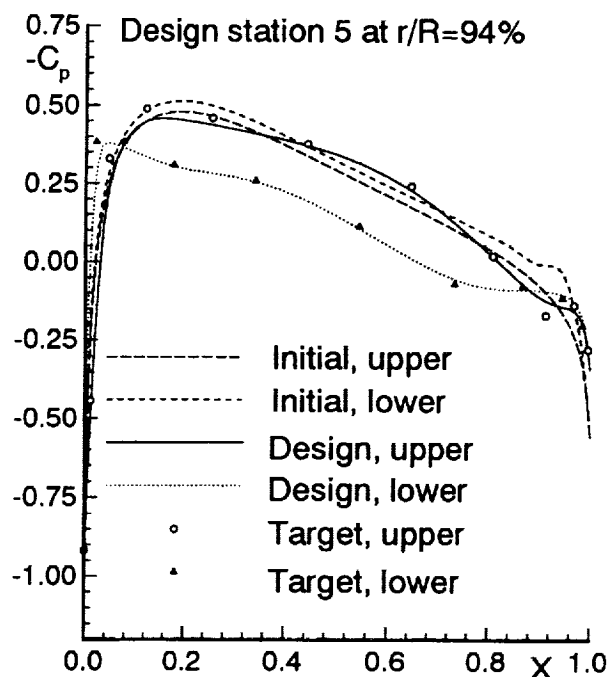
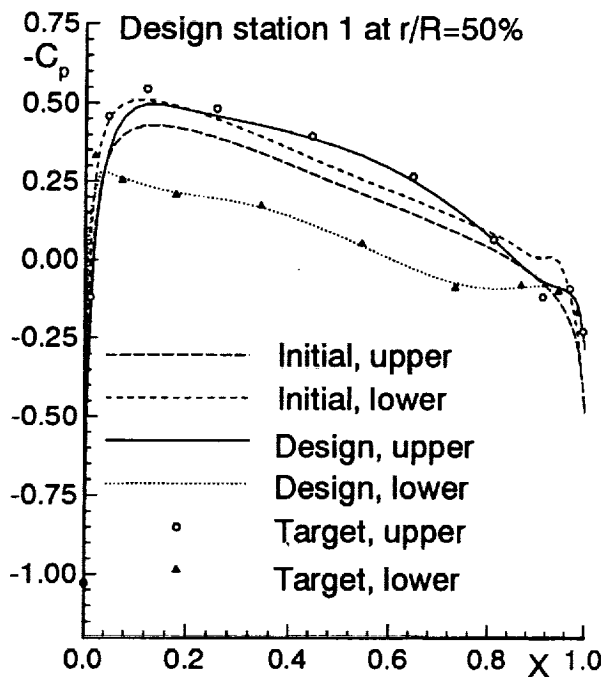


Figure 4g. Comparison of surface pressure distributions for basic DISC design case 3,  $M_{tip} = 0.95$ , where the design at cycle 50 is used.



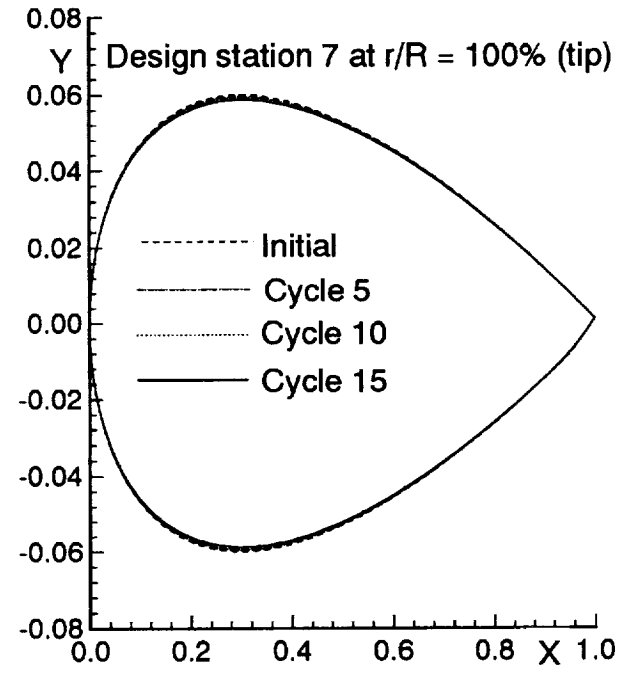
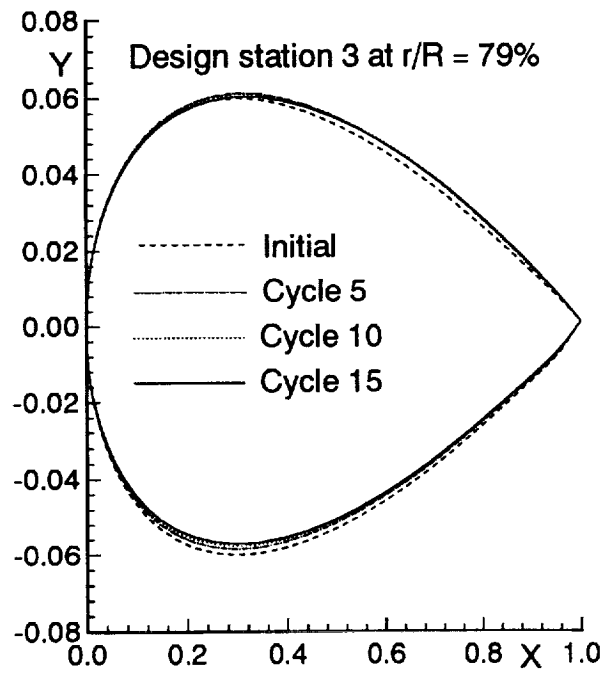
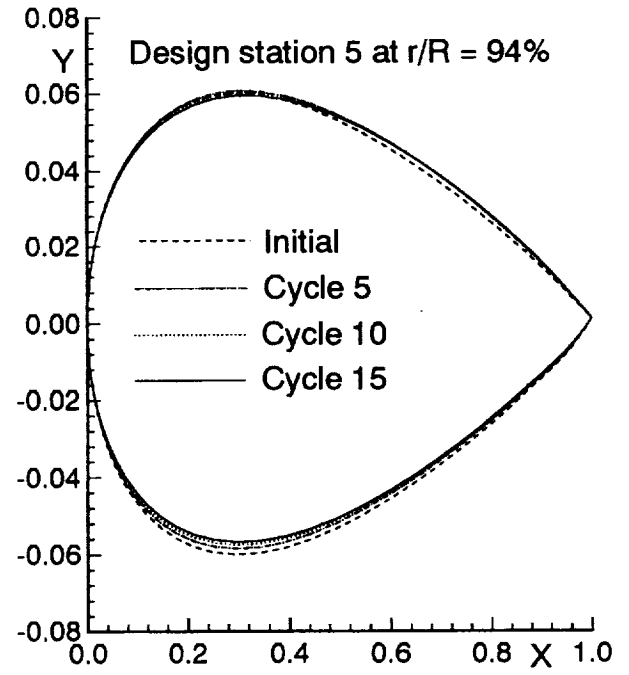
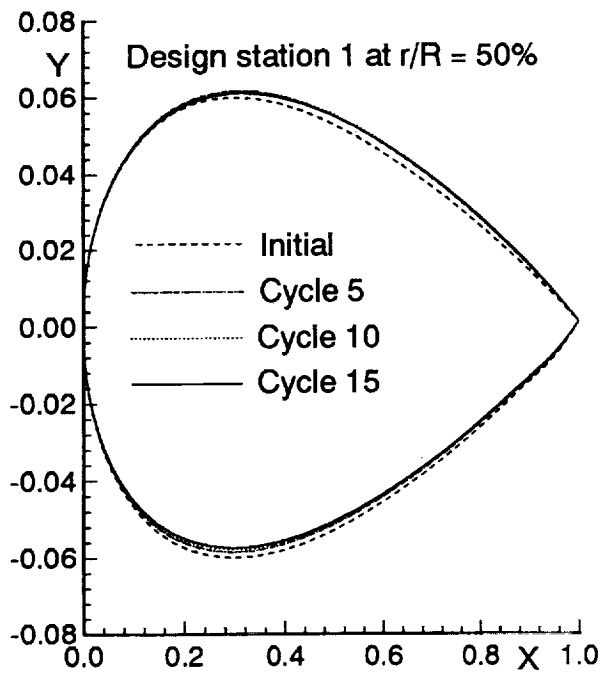


Figure 5a. Design history of blade section geometry for CDISC design case 1,  $M_{tip} = 0.95$ .

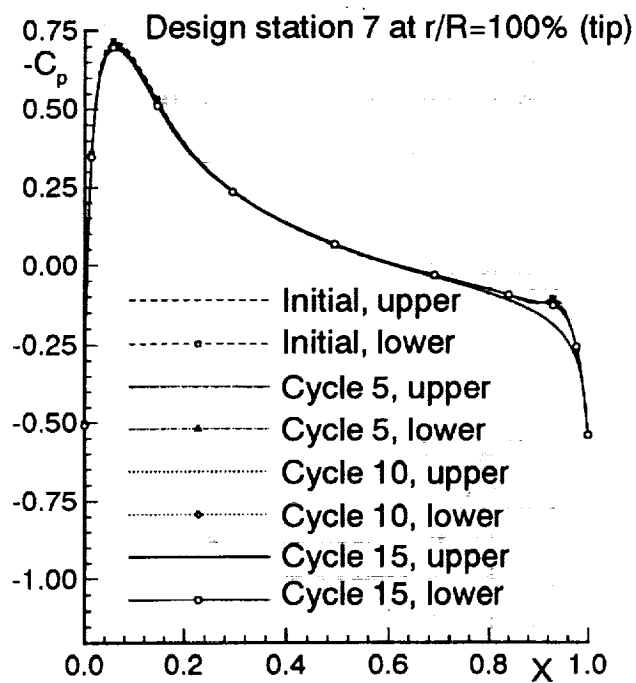
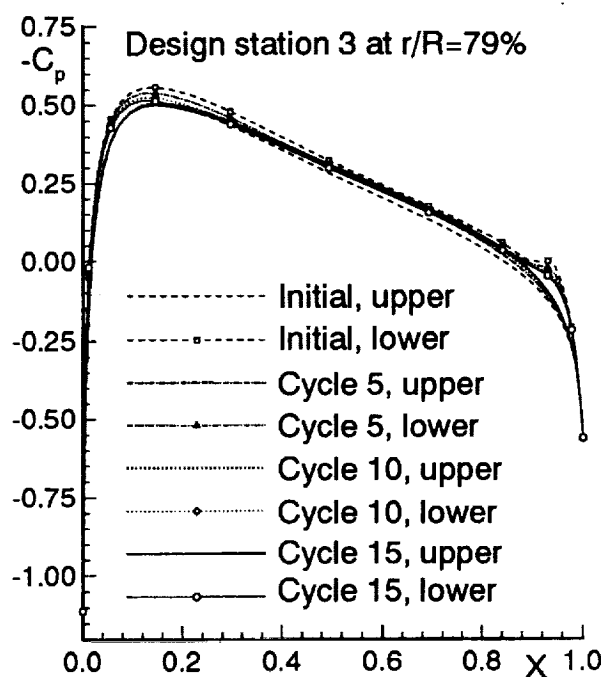
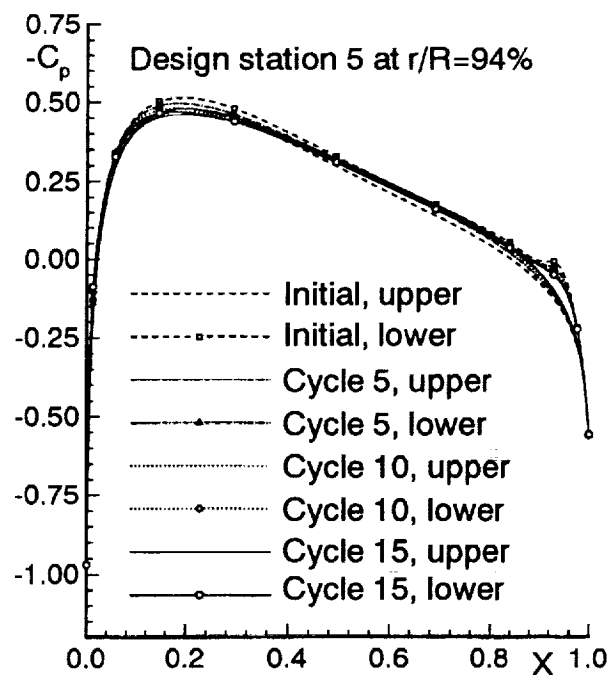
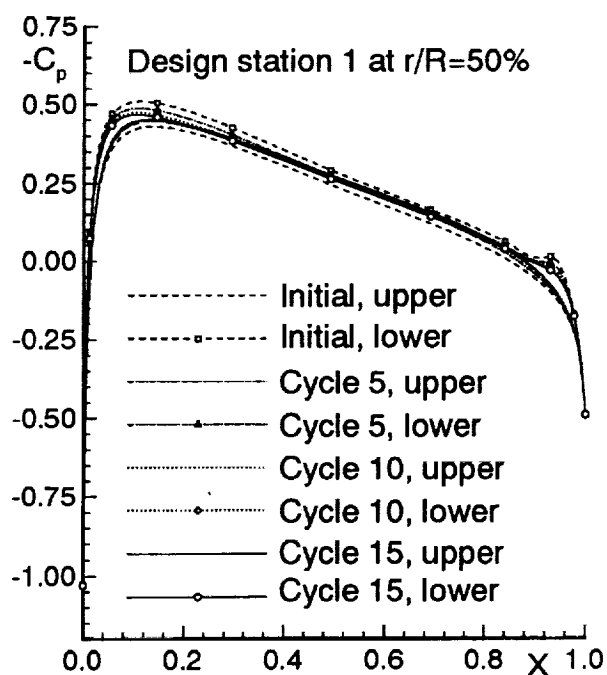


Figure 5b. Design history of surface pressure distributions for CDISC design case 1,  $M_{tip} = 0.95$ .

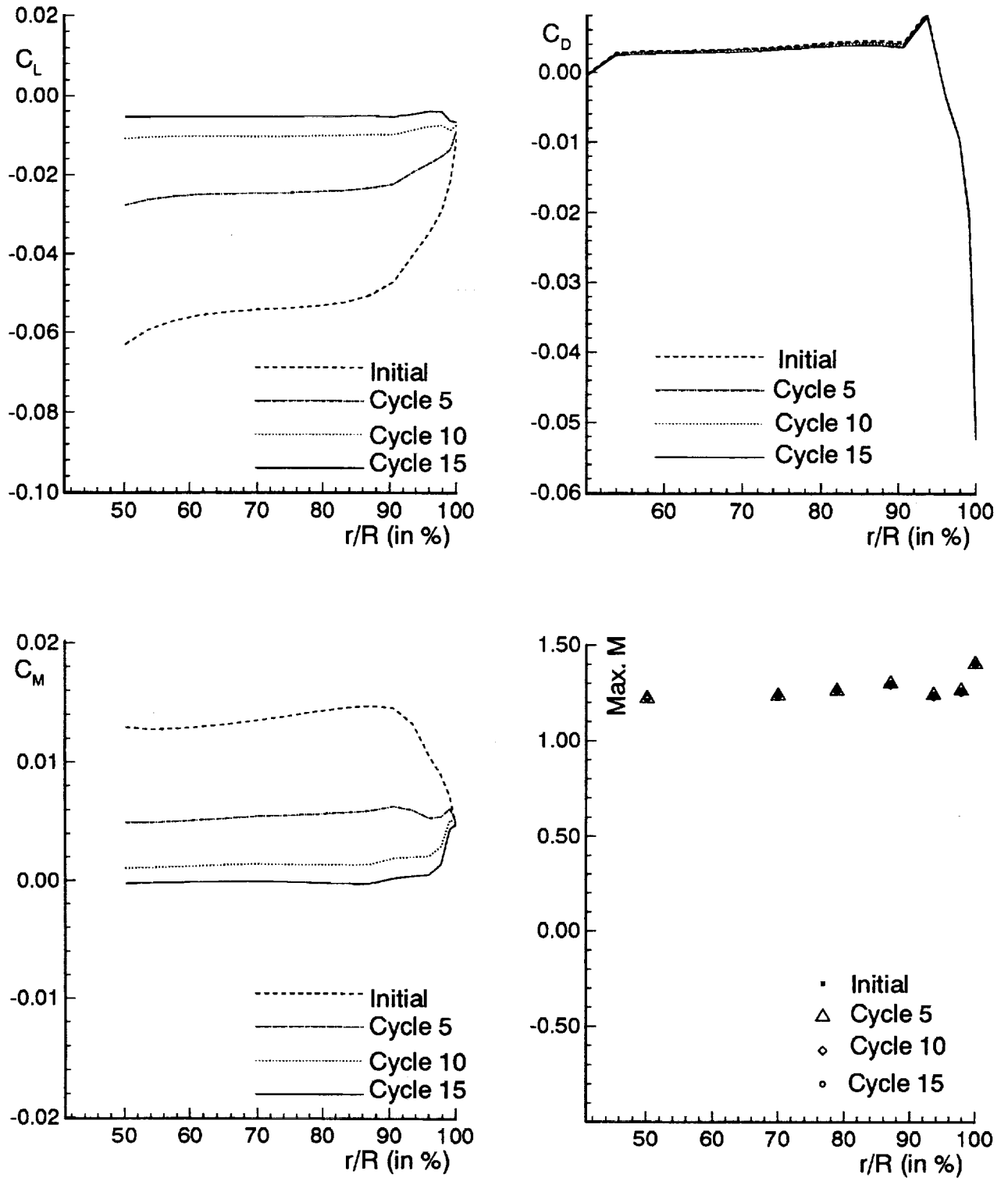


Figure 5c. Design history of spanwise lifting ( $C_L$ ), moment ( $C_M$ ), drag ( $C_D$ ) coefficients and local maximum Mach No. for CDISC design case 1,  $M_{tip} = 0.95$ .

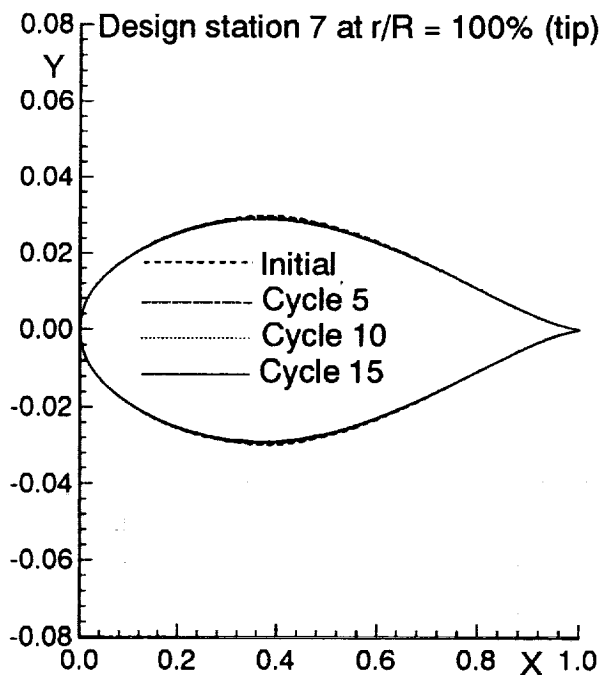
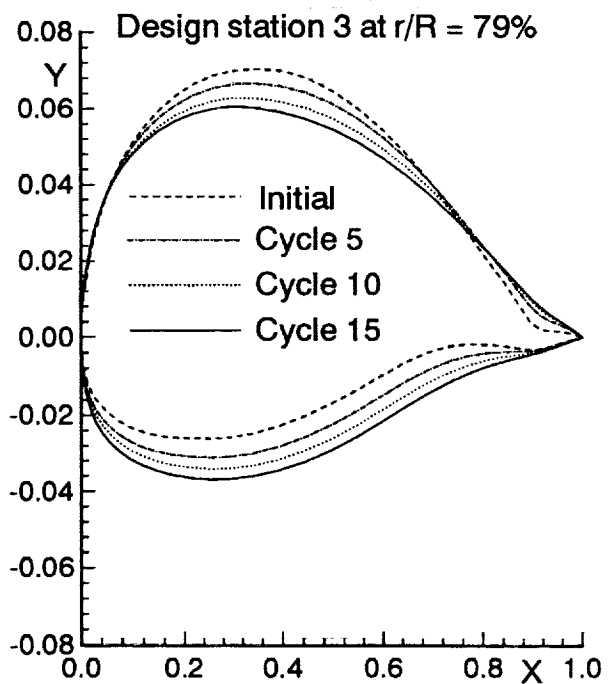
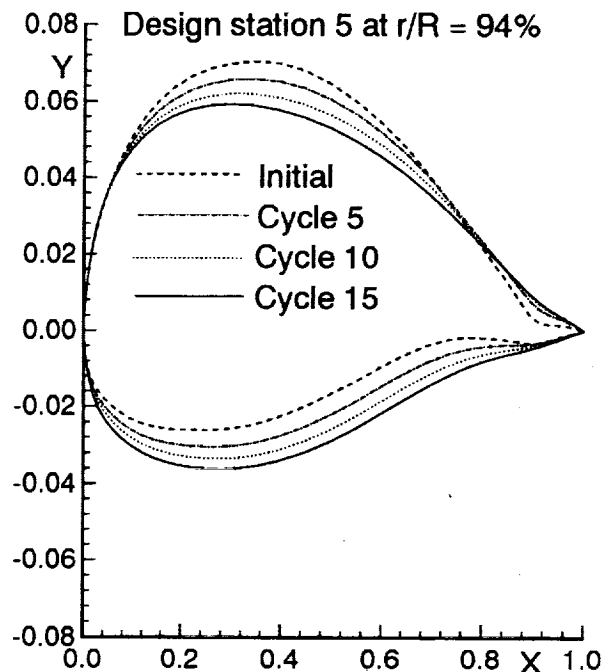
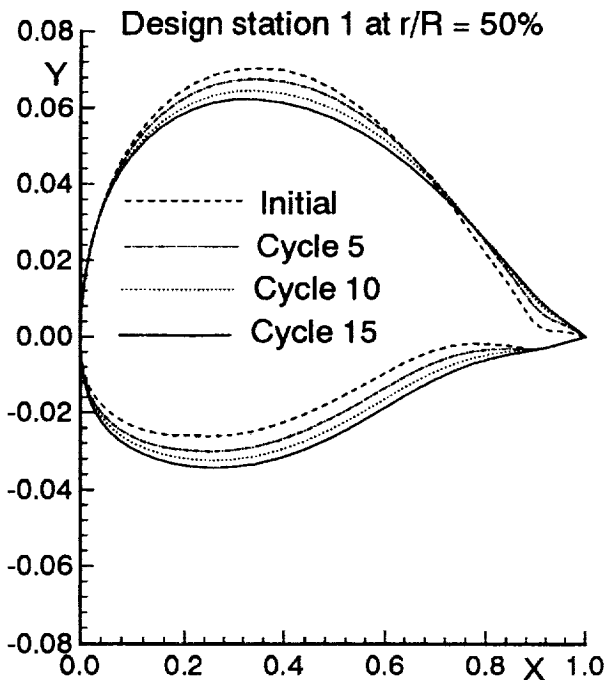


Figure 6a. Design history of blade section geometry  
for CDISC design case 2,  $M_{tip} = 0.95$ .

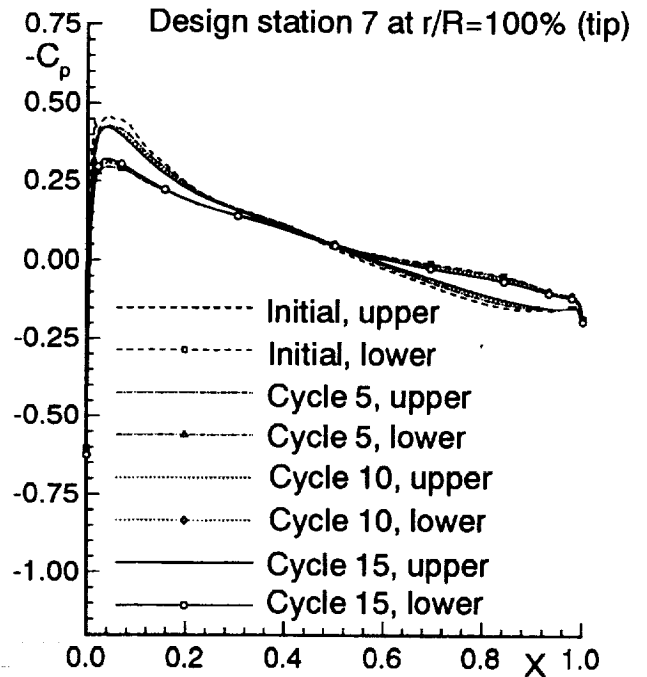
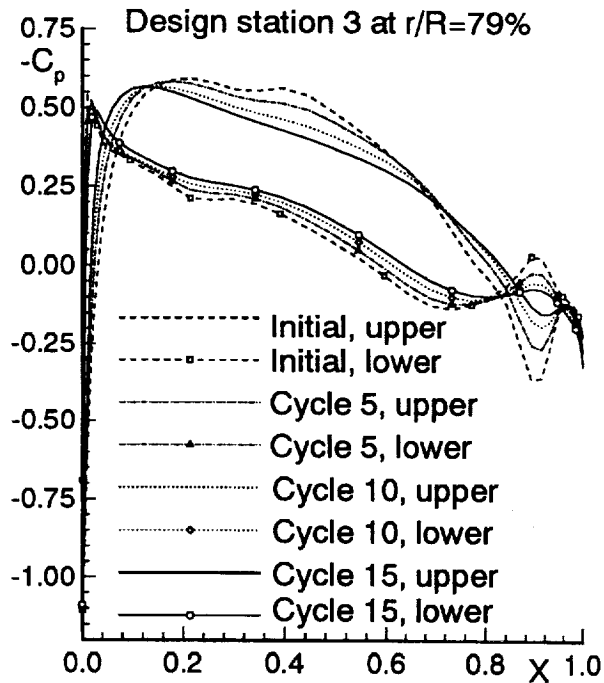
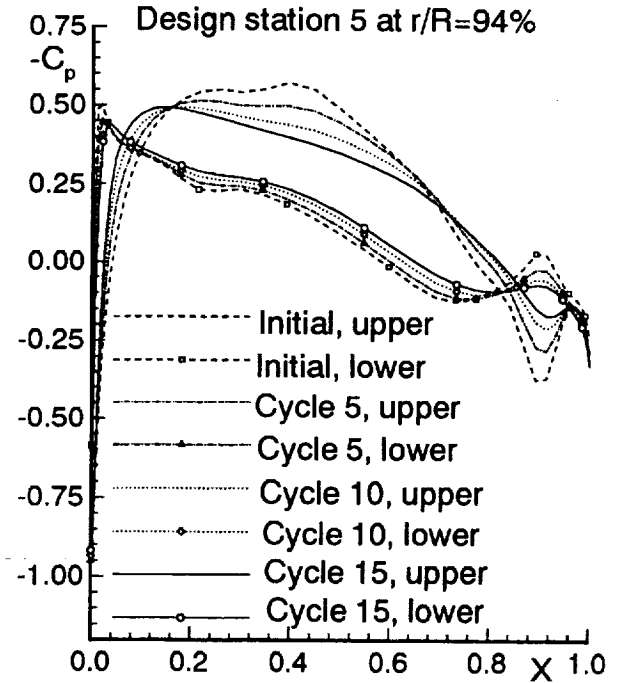
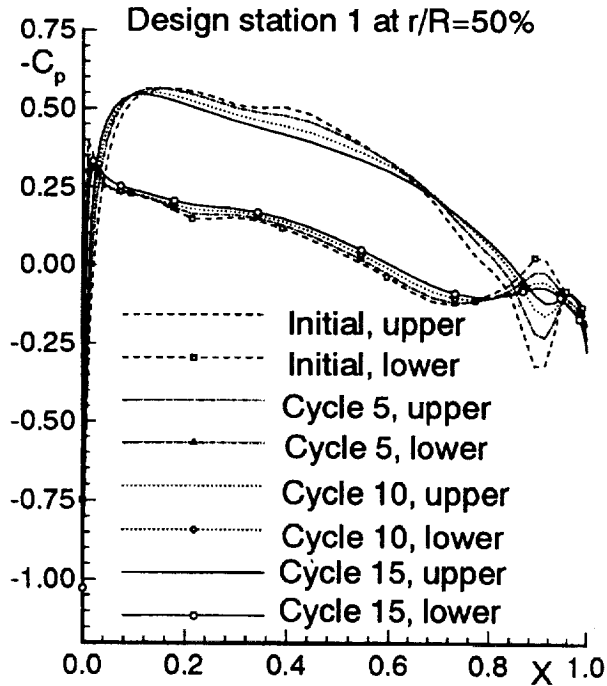


Figure 6b. Design history of surface pressure distributions for CDISC design case 2,  $M_{tip} = 0.95$ .

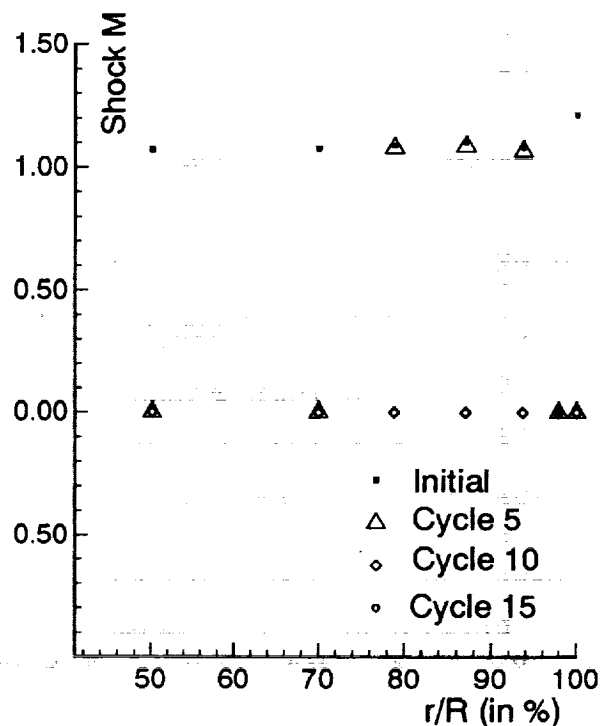
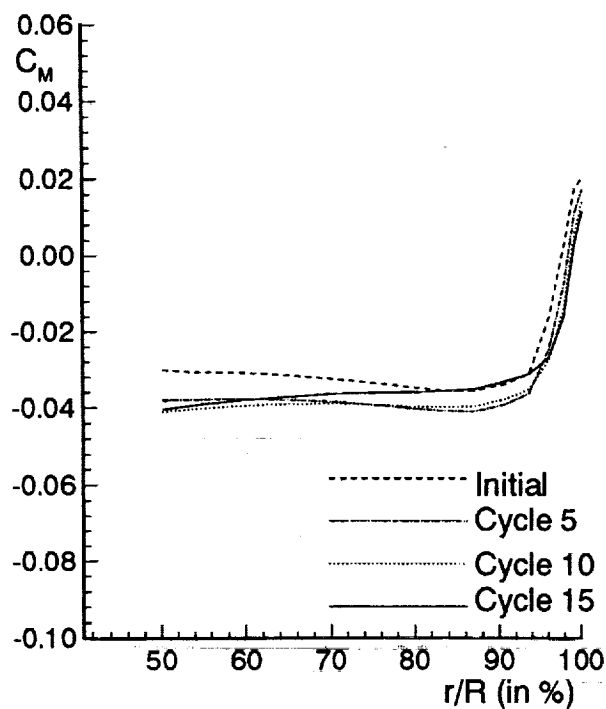
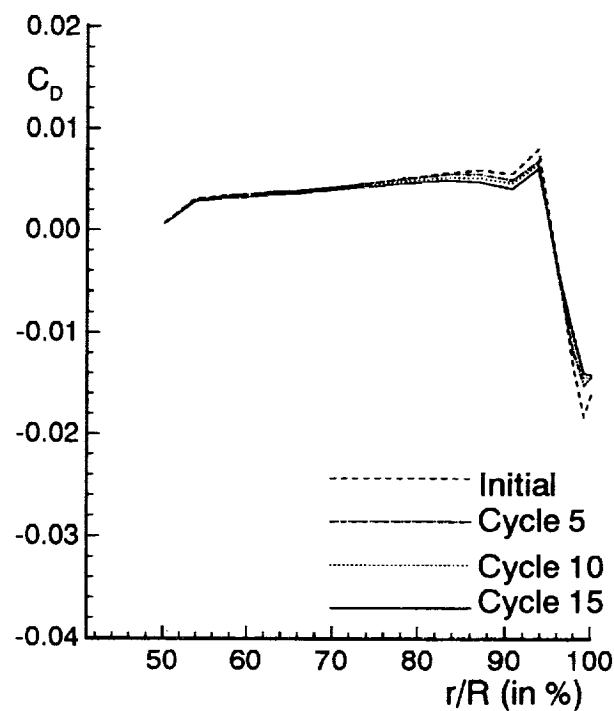
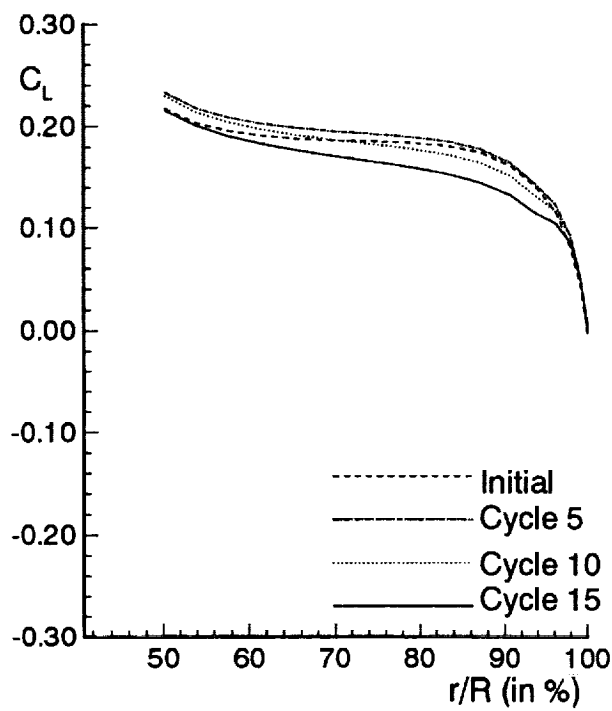


Figure 6c. Design history of spanwise lifting ( $C_L$ ), moment ( $C_M$ ), drag ( $C_D$ ) coefficients and shock Mach No. for CDISC design case 2,  $M_{tip} = 0.95$ .

## References

1. Campbell, R. L. and Smith, L. A., "A Hybrid Algorithm For Transonic Airfoil and Wing Design", AIAA Paper 87-2552, 1987.
2. Campbell, R. L., "An Approach to Constrained Aerodynamic Design With Application to Airfoils", NASA TP 3260, 1992.
3. Smith, L. A. and Campbell, R. L., "Applications of a Direct/Iterative Design Method to Complex Transonic Configurations", NASA TP 3234, 1992.
4. Mineck, R. E. and Campbell, R. L., "Demonstration of Multipoint Design Procedures for Transonic Airfoils, AIAA Paper 93-3114, 1993.
5. Campbell, R. L., "Efficient Constrained Design Using Navier-Stokes Codes", AIAA Paper 95-1808, 1995.
6. Bridgeman, J. O., Prichard, D. and Caradonna, F. X., "The Development of A CFD Potential Method for The Analysis of Tilt-Rotors", the Proceedings of the AHS Technical Specialists Meeting on Rotorcraft Acoustics and Fluid Dynamics, Philadelphia, PA, October 15-17, 1991.
7. Strawn, R. and Caradonna, F. X., "Conservative Full-Potential Model for Unsteady Transonic Rotor Flows", AIAA Journal, Vol. 25, No. 2, 1987, pp. 193-198.
8. Caradonna, F. X., Strawn, R. C. and Bridgeman, J. O., "An Experimental and Computational Study of Rotor-Vortex Interactions", the Proceedings of the Fourteenth European Rotorcraft Forum, Milano, Italy, September 20-23, 1988.
9. Purcell, T., "A Prediction of High-Speed Rotor Noise", AIAA Paper -89-1130, presented at the AIAA 12th Aeroacoustics Conference, San Antonio, Texas, April 10-12, 1989.
10. Strawn, R. C. and Bridgeman, J. O., "An Improved Three-Dimensional Aerodynamics Model for Helicopter Airloads Prediction", the AIAA 29th Aerospace Sciences Meeting, Reno, Nevada, January 7-10, 1991.
11. Bridgeman, J. O., Ramachandran, K., Caradonna, F. X. and Prichard, D., "A Computational Analysis of Parallel Blade-Vortex Interactions Using Vorticity Embedding", the Proceedings of the 50th AHS Annual Forum, Washington, DC, May 11-13, 1994, pp. 1197-1210.
12. Hu, H., "Development of an Automatic Differentiation Version of the FPX Rotor Code", Technical Report, NAS-1-19935-T11, Hampton University, Hampton, Virginia, 1996.

REPORT DOCUMENTATION PAGE			Form Approved OMB No. 0704-0188	
Public reporting burden for this collection of information is estimated to average 1 hour per response, including the time for reviewing instructions, searching existing data sources, gathering and maintaining the data needed, and completing and reviewing the collection of information. Send comments regarding this burden estimate or any other aspect of this collection of information, including suggestions for reducing this burden, to Washington Headquarters Services, Directorate for Information Operations and Reports, 1215 Jefferson Davis Highway, Suite 1204, Arlington, VA 22202-4302, and to the Office of Management and Budget, Paperwork Reduction Project (0704-0188), Washington, DC 20503.				
1. AGENCY USE ONLY (Leave blank)		2. REPORT DATE December 2000		3. REPORT TYPE AND DATES COVERED Contractor Report
4. TITLE AND SUBTITLE On the Coupling of CDISC Design Method With FPX Rotor Code			5. FUNDING NUMBERS  NAS1-19935  WU 505-598-705	
6. AUTHOR(S) Hong Hu				
7. PERFORMING ORGANIZATION NAME(S) AND ADDRESS(ES) Hampton University Hampton, Virginia			8. PERFORMING ORGANIZATION REPORT NUMBER	
9. SPONSORING/MONITORING AGENCY NAME(S) AND ADDRESS(ES) National Aeronautics and Space Administration Langley Research Center Hampton, VA 23681-2199			10. SPONSORING/MONITORING AGENCY REPORT NUMBER  NASA/CR-2000-210314	
11. SUPPLEMENTARY NOTES Langley Technical Monitor: Henry E. Jones				
12a. DISTRIBUTION/AVAILABILITY STATEMENT Unclassified-Unlimited Subject Category 70      Distribution: Nonstandard Availability: NASA CASI (301) 621-0390			12b. DISTRIBUTION CODE	
13. ABSTRACT (Maximum 200 words) The rotor section aerodynamics design package is developed by coupling Constrained Direct Iterative Surface Curvature (CDISC) design method with the FPX rotor code. The coupling between the CDISC design and the FPX flow analysis is fully automated. The CDISC design method employs a predictor-corrector procedure iteratively to determine a surface geometry which produces a target pressure distribution, where the target pressure distributions is either pre-defined or automatically generated through flow and geometry constraints. The FPX code is an eXtended Full-Potential rotor Computational Fluid Dynamics (CFD) code, which solves the three-dimensional unsteady full-potential equation in a strong conservative form using an implicit approximate-factorization finite-difference scheme with entropy and viscosity corrections. Application of the CDISC design method coupled with the FPX rotor code is made for rotor blades in hovering motions. Several design examples are presented to demonstrate the capability of the new package in rotor section design.				
14. SUBJECT TERMS Rotorcraft; CFD; Sensitivity Analysis; Design			15. NUMBER OF PAGES 40	
			16. PRICE CODE A03	
17. SECURITY CLASSIFICATION OF REPORT Unclassified	18. SECURITY CLASSIFICATION OF THIS PAGE Unclassified	19. SECURITY CLASSIFICATION OF ABSTRACT Unclassified	20. LIMITATION OF ABSTRACT UL	